Biocatalytic Synthesis of Furan-Based Oligomer Diols with Enhanced End-Group Fidelity

Skoczinski, Pia; Cangahuala, Monica K. Espinoza; Maniar, Dina; Albach, Rolf W.; Bittner, Natalie; Loos, Katja

Published in:
ACS Sustainable Chemistry & Engineering

DOI:
10.1021/acssuschemeng.9b05874

ACS Sustainable Chemistry & Engineering

Research Article

Cite This: ACS Sustainable Chem. Eng. 2020, 8, 1068−1086

pubs.acs.org/journal/ascecg

Biocatalytic Synthesis of Furan-Based Oligomer Diols with Enhanced End-Group Fidelity

Pia Skoczinski,[†,§] Mónica K. Espinoza Cangahuala,[†] Dina Maniar,[†] Rolf W. Albach,[‡] Natalie Bittner,[‡] and Katja Loos*[,†]

[†]Macromolecular Chemistry and New Polymeric Materials, Zernike Institute for Advanced Materials, University of Groningen, Nijenborgh 4, 9747 AG Groningen, The Netherlands

[‡]Covestro Deutschland AG, Kaiser-Wilhelm-Allee 60, 51373 Leverkusen, Germany

ABSTRACT: The lipase-catalyzed synthesis of furan-comprising polyester oligomer diols (α,ω-telechelic diols) is reported. Oligofuranoate diols with excellent end-group fidelity and a yield of 95% were synthesized using a solvent-free two-stage polycondensation of dimethyl furan-2,5-dicarboxylate (DMFDCA) and 1,4-cyclohexanedimethanol (1,4-CHDM) using immobilized *Candida antarctica* Lipase B (CalB). Recycling of immobilized CalB to further decrease the production cost is successfully demonstrated. However, it showed limitation in the product yield that decreases ±20% with each additional reuse. The synthetic procedure has been scaled up, easily opening the possibility to use the developed diols in industrial polycondensations utilizing the excellent flame retardancy property and high thermal stability typical for furan-based polymers.

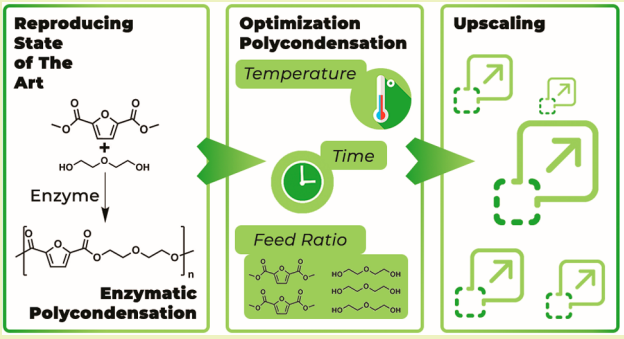

KEYWORDS: *Furan-based polymers, Polyester, Oligomer diols, Enzymatic polymerization, End-group fidelity*

INTRODUCTION

Increasing CO_2 emissions and climate change have led to a rethinking of industrial production of chemicals and pharmaceuticals. Therefore, ideas and principles have been developed to reduce environmental pollution, conserve energy, and produce in an environmentally friendly way.[1−3] Various product syntheses are more and more based on monomers gained from renewable resources. These monomers or building blocks are produced from biomass feedstocks via sugar or biobased syngas intermediates and are used for various applications as polymer synthesis, emulsifier generation, amine synthesis, or solvent production.

Hydroxymethylfurfuraldehyde (HMF) is a furan derivative that can be prepared from C6 polysaccharides or sugars.[4−7] The conversion of fructose to HMF is, for example, performed by acid-catalyzed dehydration in water with phase modifiers,[8] supercritical acetone,[9] or high boiling point solvents.[10] HMF has received some attention because of its oxidation product, 2,5-furandicarboxylate (FDCA), which is considered as a suitable alternative to terephthalic acid (TPA) and isophthalic acid.[11−22] In general, two synthesis approaches were developed as the main fashion in furan-based polymers. In the first approach, a Diels−Alder reaction is applied to synthesize novel thermally reversible polymers from furan/maleimide and diene/dienophile combinations, while the second approach is via a polycondensation reaction and involves mostly monomers related to FDCA. A comprehensive review on the furan-based polymers from the first approach has been published by Gandini et al.[23]

Furans are also of interest for industrial commodity polymers such as polyurethanes (PU) because they might provide improved flame retardant properties when incorporated.[24,25] For instance, Guo et al. recently reported on the excellent flame retardancy property and high thermal stability of novel difuranic diepoxide monomers and the respective epoxy/amine thermosetting resins.[26] While flame retardants are available for use today to lower the fire risk of, for instance, PU foams, some of these flame retardants of small molecular size have been found to have environmental persistence issues, as well as negative bioaccumulation and toxicity profiles.[27−30] Reactive flame retardants are those chemicals which are covalently incorporated into the polymer synthesis and cannot leach out of the polymer over time.[31−33] Further, they are intimately mixed with the polymer during burning, can activate immediately in a fire, and will always be available for protection since they cannot be removed like a conformal coating or damaged like a barrier fabric. Furan-based oligomer diols could be ideal reactive flame retardants as building blocks for polycondensates such as polyurethanes but also polyester, polyesteramides, etc.

Diol derivatives (α,ω-telechelic diols) are especially targeted due to the feasibility of the hydroxyl end groups to react with different functional groups.[34−36] At this point oligomer diols are industrially mainly synthesized via depolymerization routes.

Received: October 3, 2019
Revised: November 18, 2019
Published: December 2, 2019

DOI: 10.1021/acssuschemeng.9b05874
ACS Sustainable Chem. Eng. 2020, 8, 1068−1086

Polyethylene terephthalate (PET) oligomeric diols are frequently produced by depolymerization via glycolysis.[37−41] This process is used to upgrade recycled PET via postcondensation of PET diols. Another prominent example is poly(ε-caprolactone) (PCL) diol for biomedical applications. It can be easily synthesized via ring-opening polymerization (ROP) of ε-caprolactone (CL) using a diol as the initiator/chain-transfer agent in the presence of a catalyst.[42]

The current reported oligomeric diols are mainly synthesized under harsh conditions with high temperature, low pH, Lewis acids, and high pressure. These syntheses often result in low catalytic efficiency and lack enantiomeric specificity for synthesis of, for example, chiral molecules.[43] Specifically, furans are highly temperature sensitive. There is a significant risk of degradation at high temperatures that are generally used for conventional polyester oligomeric diols synthesis by polyaddition, and alternative syntheses routes need to be established. These disadvantages can been overcome with the use of microbial enzymes, which function as so-called biocatalysts.[44−48] Biocatalysts allow reaction performance with less energy and increased velocity. For industrial processes, this means that certain biochemical or biological reactions can be performed more effectively compared to conventional chemical methods regarding stereoselectivity and regioselectivity of the product. Furthermore, biocatalysts have the advantage to act under mild reaction conditions and do not need functional group protection of substrates, all resulting in fulfilling the demands of a sustainable chemistry route by decreasing waste disposal and energy costs.[43,49−60] Therefore, microbial enzymes are currently widely used in several industrial applications with leading use in chemical product synthesis, the food industry, the animal feed stuff industry, and in production of washing agents.[61] The most abundant enzyme classes in these fields are proteases, amylases, and lipases.[61]

Recently, we have reported on lipase-catalyzed polycondensation of dimethyl furan-2,5-dicarboxylate (DMFDCA) as a furan and diethylene gycol (DEG) as a diol.[62] Lipases (EC 3.1.1.3) belong to the carboxylester hydrolases subgroup (EC 3.1.1), and together with esterases (EC 3.1.1.1), lipases are able to hydrolyze and transesterify ester bonds. Here, lipases also named triacylglycerol hydrolases are known to act on lipids, which means they catalyze the hydrolysis and synthesis of esters formed from glycerol and long-chain fatty acids.[63,64] The lipase used in our recent work is *Candida antarctica* lipase B (CalB). Due to its broad substrate specificity, high regio-, stereo-, and enantioselectivity, high activity in organic solvents and at elevated temperatures, CalB is the most commonly used lipase in organic and polymer chemistry.[65] It is also used for the industrial purpose of its natural catalysis of fat and oil processing.[65] Regarding organic chemistry and polymer chemistry, CalB is able to convert simple alcohols and carbohydrates to different kind of esters[65] and is commonly used for generating polymers that comprise monomers with sensitive groups that cannot be synthesized using conventional chemical routes[66−68] or for a nearly complete green chemistry route to catalyze the generation of biobased polyesters and polyamides.[69−81]

Enzymatic polymerization/oligomerization can therefore be considered an ideal method to synthesize α,ω-telechelic furan-based diols. Here, we report on the lipase-catalyzed synthesis of furan-comprising oligomer diols with a high end-group fidelity. Our previous reported method was optimized in terms of monomeric diols used, solvent systems, time, and temperature to increase the yield and to obtain a majority of OH/OH end groups. Additional focus was put on rendering the developed method more industrially viable (replacement of organic solvents, recycling of biocatalysts, scale up, etc.).

MATERIALS AND METHODS

Phosphorus pentoxide, desiccant with moisture indicator (CAS number: 1314-56-3), diphenyl ether, HPLC grade (CAS number: 101-84-8), diethylene glycol (CAS number: 111-46-6), 1-butanol (CAS number: 71-36-3), 1,4-butanediol (CAS number: 110-63-4; 99% pure), Chloroform-d (CAS number: 865-49-6), Chloroform, CHROMASOLV amylene stabilized (CAS number: 67-66-3), 1,4-cyclohexanedimethanol (cis/trans mixture; CAS number: 105-08-8; 99% pure), *Candida antarctica* lipase B on acrylic resin (CalB, Novozym435, 5000 + U/g; CAS number: 9001-62-1), and molecular sieves (4 Å, CAS number: 70955-01-0) were purchased from Sigma-Aldrich. Dimethyl furan 2,5-dicarboxylate (CAS number: 4282-32-0) was purchased from Fluorochem. Chloroform, ChromAR (CAS number: 64-66-3) was purchased from Macron Fine Chemicals. Diethyl ether (butylated hydroxytoluene (BHT) stabilized) (CAS number: 60-29-7) was purchased from Biosolve. Lewatit beads (Lewatit VP OC 1600) were obtained from Lanxess. Folded filters, grade: 15, 65 g/m^2, were purchased from Munktell Ahlstrom. Whatman filter papers, 40, for vacuum filtration were purchased from GE Healthcare Life Sciences. Acetonitrile, HPLC-S grade (CAS number: 75-05-8) was purchased from Biosolve. Formic acid for mass spectrometry (CAS number: 64-18-6) was purchased from Honeywell, and ammonium hydroxide solution, ≥25% NH3 in H_2O, semiconductor grade PURANAL (CAS number: 1336-24-6) was purchased from Sigma-Aldrich.

General Procedure for CalB-Catalyzed Polycondensation of Dimethyl Furan-2,5-dicarboxylate and Different Diols via a Two-Stage Method. CalB was predried for 24 h in the presence of phosphorus pentoxide (P_2O_5) at room temperature under high vacuum. Diphenyl ether was vacuum distilled and stored with 4 Å molecular sieves under a nitrogen environment.

Dimethyl furan-2,5-dicarboxylate (DMFDCA), the diol, predried CalB or predried Lewatit beads (for the negative control reaction), and in the solvent system also distilled diphenyl ether were added into a 25 mL round-bottomed flask. The DMFDCA and the corresponding diol were applied in a total concentration of 10.8608 mmol; the amount of diphenyl ether, if used, and the amount of predried CalB were calculated based on this total monomer amount. The different monomer ratios (with a total concentration of 10.8608 mmol) and different reaction times and temperatures, as well as the different enzyme amounts used are mentioned in detail in the Results and Discussion section. The reaction was magnetically stirred at 130 rpm in an oil bath. A two-stage method was applied for enzymatic polycondensation. In the first stage, the reaction was performed at temperatures varying from 80 to 140 °C for 2 h under an atmospheric nitrogen environment. In the second stage, polycondensation was performed at temperatures varying from 80 to 140 °C under reduced pressure of 2 mmHg for an additional time of 24 to 72 h.

After polycondensation in the solvent or the solvent-free system, 20 mL of chloroform was added into the reaction flask and stirred at room temperature and 450 rpm for 1 h to stop the reaction and to dissolve the polycondensation products. CalB was filtered off by filtration, and the round-bottomed flask was washed three times with 15 mL chloroform. For recovery (precipitation) of the oligofuranoates generated via the solvent system, the oligomer solution was added dropwise under constant stirring (450 rpm) into a 10-fold excess of ice-cold diethyl ether. The diethyl ether solution with the precipitated oligofuranoates was first stirred at room temperature and 450 rpm for 1 h and then stored overnight at −20 °C. Subsequently, the precipitated oligofuranoates were collected by vacuum filtration and washed three times with ice-cold diethyl ether. Concerning the oligomers synthesized via the solvent-free system, the oligofuranoate solutions were concentrated by evaporating the chloroform at 40 °C under reduced pressure (356 mmHg). After drying of the oligomers in a vacuum oven at room temperature overnight, the generated oligofuranoates were

DOI: 10.1021/acssuschemeng.9b05874
ACS Sustainable Chem. Eng. 2020, 8, 1068−1086

analyzed by ^{1}H NMR measurement for validation of oligomer formation.

Recycling of Immobilized CalB. For recycling, immobilized CalB was used in two different ways: without washing and with washing. For without washing, immobilized CalB was dried at room temperature overnight under atmospheric pressure after the general solving, filtration, and washing procedure and reused for another polycondensation. For with washing, immobilized CalB was additionally to the general procedure, washed three times with 10 mL of 1-butanol and subsequently dried at room temperature overnight under atmospheric pressure and reused for another polycondensation.

Molecular Weight Analysis of the Obtained Oligofuranoates. For the molecular weight determination of the produced oligofuranoates, two methods were applied. Calculation of the number-average molecular weight oligomer $\overline{M_n}$ by analysis of the ^{1}H NMR spectra[82] and calculation of $\overline{M_n}$ and the weight-average molecular weight $\overline{M_w}$ by gel permeation or size exclusion chromatography, subsequently also the dispersity $Đ$ of the oligofuranoates could be determined by $\overline{M_w}/\overline{M_n}$.

NMR Analysis. *^{1}H NMR measurement.* ^{1}H NMR and ^{13}C NMR spectra were recorded on a Varian VXR spectrometer (400 MHz for ^{1}H NMR and 100 MHz for ^{13}C NMR analysis), using $CDCl_3$-d_1 as the solvent. For NMR spectra evaluation, the software MestReNova (Version: 6.0.2-5475) was used. The chemical shifts reported were referenced to the resonance of $CDCl_3$-d_1.

NMR Analysis of the Generated Poly (Diethylene Glycol Furanoate). **^{1}H NMR** (400 MHz, $CDCl_3$-d_1, ppm): 7.260 $CDCl_3$-d_1 7.18 (2H, s, −C***H***=, furan), 4.47 (4H, t, −CO−O−C***H***$_2^-$, from DEG), 3.83 (4H, t, −C***H***$_2$−O−C***H***$_2^-$, from DEG), 3.91 (s, −OC***H***$_3$, end group from DMFDCA), 3.74 (m, −CO−O−CH$_2$−C***H***$_2$−OH, end group from DEG), 3.64 (m, −O−C***H***$_2$−CH$_2$−OH, end group from DEG), 2.43 (m, −O***H***, end group from DEG).

^{13}C NMR (100M Hz, CDCb-d1, ppm). 77.36 CDC1rd 157.79 (−C=O), 146.57 (=C(C)−0−, furan), 118.68 (=**C**−, furan), 68.82 (−CHrO−CHr), 64.27 (−C0−0−CHr), 72.47 (−0−CHrCHrOH, end group), 61.67 (−0−CHrCHrOH, end group), 52.39 (−O− CH3, end group from DM FDCA).

NMR Analysis of the Generated Poly(butylene) Furanoate. ***^{1}H NMR** (400 MHz, $CDCl_3$-d_1, ppm): 7.260 $CDCl_3$-d_1.* 7.21 (2H, s, −C**H**═ cyclo, from DMFDCA), 4.40 (2H, t, −CO−O−C**H**$_2$−CH$_2$−CH$_2$−CH$_2$−OH, from 1,4-BDO), 3.93 (3H, s, −OC**H**$_3$, end group from DMFDCA), 3.70 (2H, t, −CO−O−CH$_2$−CH$_2$−CH$_2$−C**H**$_2$−OH, end group from 1,4-BDO), 1.98 (2H,m, −CO−O−CH$_2$−C**H**$_2$−CH$_2$−CH$_2$−OH, from 1,4-BDO), 1.91 (2H, m, −CO−O−CH$_2$−CH$_2$−C**H**$_2$−CH$_2$−OH, from 1,4-BDO), 1.58 (1H, s, −CO−O−CH$_2$−CH$_2$−CH$_2$−CH$_2$−O**H**, end group from 1,4-BDO).

NMR Analysis of the Generated Poly(methoxycyclohexyl) Furanoate. ***^{1}H NMR** (400 MHz, $CDCl_3$-d_1, ppm): 7.260 $CDCl_3$-d_1.* 7.21 (2H, s, −C**H**═cyclo, from DMFDCA), 4.28/4.18 (4H, 2d, −CO−O−C**H**$_2$−(CH−cyclo−CH)−CH$_2$−OH, from 1,4-CHDM), 3.93 (3H, s, −OC**H**$_3$, end group from DMFDCA), 3.55/3.48 (4H, 2d, −CO−O−CH$_2$−(CH−cyclo−CH)−C**H**$_2$−OH, end group from 1,4-CHDM), 2.0 (2H, s, −CO−O−CH$_2$−(C**H**−cyclo−C**H**)−CH$_2$−OH, ring structure from 1,4-CHDM), 1.90−1.48/1.16−0.99 (8H, 2m, −CO−O−CH$_2$−(CH−**cyclo**−CH)−CH$_2$−OH ring structure from 1,4-CHDM), not visible (−CO−O−CH$_2$−(CH−cyclo−CH)−CH$_2$−O**H** end group from 1,4-CHDM).

^{13}C NMR (100 MHz, $CDCl_3$-d_1, ppm): 77.360 $CDCl_3$-d_1. 158.12 (−**C**O−O, from DMFDCA), 146.91 (O−**C**−CO−O, from DMFDCA), 118.26 (−**C**H═cyclo, from DMFDCA), 70.31/70.12 (−CO−O−CH$_2$−(CH−cyclo−CH)−**C**H$_2$−OH, from 1,4-CHDM), 68.60/66.20 (−CO−O−**C**H$_2$−(CH−cyclo−CH)−CH$_2$−OH, from 1,4-CHDM), 52.41 (−O**C**H$_3$, end group from DMFDCA), 40.58/40.29 (−CO−O−CH$_2$−(CH−cyclo−**C**H)−CH$_2$−OH, from 1,4-CHDM), 37.20/37.02 (−CO−O−CH$_2$−(**C**H−cyclo−CH)−CH$_2$−OH, from 1,4-CHDM), 28.91/28.69/25.44/25.30/25.07 (−CO−O−CH$_2$−(CH−**cyclo**−CH)−CH$_2$−OH, from 1,4-CHDM).

Molecular Weight Calculation by ^{1}H NMR Spectroscopy.[82] First, the number of repeating units n was determined via eq 1.

$$\frac{\sum a_{\text{repeating unit}} \times m_{\text{furan end group}} \times n_{\text{furan end group}}}{a_{\text{end group}} \times \sum m_{\text{repeating unit}}} = n \quad (1)$$

The number of repeating units n was then multiplied with the molecular weight of the repeating unit of the corresponding oligomer leading $\overline{M_n}$, the number-average molecular weight. The molecular weight of the poly(butylene) furanoate repeating unit is 210.18 and 264.27 g/mol for the poly(methoxycyclohexyl) furanoate repeating unit. For the oligomers generated via the solvent system the furan end group, −OC**H**$_3$ (3.93 ppm) was used as a reference for determining the repeating units. For oligomers synthesized in the solvent-free system, the 1,4-cyclohexanedimethanol end group −C**H**$_2$OH (3.5 and 3.47 ppm) was used as a reference.

Gel Permeation Chromatography (GPC). For gel permeation chromatography (GPC)/size exclusion chromatography (SEC), the generated oligofuranoates were diluted in Chloroform, CHROMASOLV for HPLC to a final concentration of 3 mg/mL. Measurement of each sample was performed twice at 30 °C using a Viscotek SEC (Malvern, Germany) and a PLgel MIXED-C column (5 μm, 200 mm) (Agilent Technologies, USA). Chloroform, CHROMASOLV for HPLC was used as the eluent with a flow rate of 1 mL/min. Subsequent molecular weight calculations were performed with OMNISEC software (Malvern, Germany) based on the conventional calibration method using the conventional calibration curve generated by polystyrene standards (Agilent Technologies, USA) with $\overline{M_w}$ ranging from 655 to 3001000 g/mol.

Thermal Analysis of the Obtained Oligofuranoates. Thermal properties of the produced oligofuranoates were analyzed by thermal gravimetric analysis (TGA) for determining thermal stability and decomposition within a specific temperature range and by differential scanning calorimetry (DSC) for melting and crystallinity behavior. Evaluation for both measurements was performed using the TRIOS v4.3.0 software from TA Instruments.

Thermal Gravimetric Analysis (TGA). Thermal stability and decomposition of the oligofuranoates were determined using the TGA5500 (TA Instruments, USA). In a first step, the samples with a concentration from 1 to 5 mg were heated to 120 °C (10 °C/min) and kept isothermal for 30 min to remove residual solvent. Afterward, the temperature was increased from 30 to 700 °C (10 °C/min). All steps were performed under nitrogen atmosphere.

Differential Scanning Calorimetry (DSC). The melting and crystallinity behavior of the oligofuranoates was analyzed with the DSCQ1000 (TA Instruments, USA). For determining the melting (T_m) and crystallizing temperatures (T_c), the measurement was performed from −20 to 250 °C with heating of 10 °C/min including two heating steps with two cooling steps and a subsequent temperature-modulated cycle including one heating step for determining the glass transition temperature (T_g). Also, here heating was performed from −20 to 250 °C, but the heating rate for this temperature-modulated cycle was decreased to 2 °C/min with the temperature modulated at ±0.5 °C every 60 s.

Microstructure Analysis. The different microstructures or different oligomer species within the different generated oligofuranoates were identified via electro spray ionization high resolution mass spectrometry (ESI-HRMS). The oligofuranoate species with different end groups were identified by combining the experimental data from ESI-HRMS analysis and the predicted molecular weight of the oligofuranoate by the ChemDraw Ultra 11.0 software. The via ESI-HRMS-determined molecular weight (g/mol) (with previous subtraction of the adduct ions for ionization (18 g/mol NH_4^+ ions)) of the oligofuranoate was compared to the corresponding molecular weight-predicted structure. This way allowed for the identification of the oligofuranoate end groups. The majority of the oligofuranoates with certain end groups was determined by the measured intensity (atomic mass unit (amu)) during ESI-HRMS.

Electro Spray Ionization High Resolution Mass Spectrometry (ESI-HRMS). The oligofuranoate samples with a concentration of 1 mg were dissolved in dichloromethane and diluted 200-fold in acetonitrile with 0.1% formic acid to generate Na-adduct ions and if necessary 0.1% NH_4OH to generate NH_4-adduct ions. The dissolved and diluted

DOI: 10.1021/acssuschemeng.9b05874
ACS Sustainable Chem. Eng. 2020, 8, 1068−1086

A

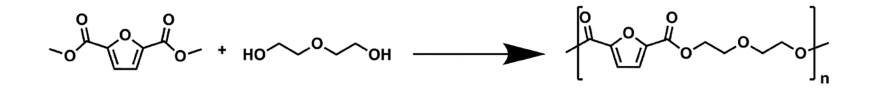

dimethyl furan-2,5-dicarboxylate diethylene glycol poly(diethylene glycol) furanoate (PDEGF)

B

parameters	1
Monomer amount	30 % of total reaction volume
Monomer ratio	2:2
Enzyme amount/Lewatit beads amount	25 wt%
Solvent	diphenyl ether
Solvent amount	380 wt %
Temperature	80 °C
Time	2/72 h
Surrounding (N_2,vacuum)	N_2/2 mmHg

Figure 1. (A) Polycondensation of dimethyl furan-2,5-dicarboxylate and diethylene glycol. (B) Experimental set up of the polycondensation.

samples were introduced to the mass spectrometry by a syringe pump with direct infusion using a flow rate of 10 μL/min. The spectra were acquired with electrospray ionization in a scan range from 75 to 2500 amu in the positive ion mode on the maXis plus mass spectrometer (Bruker, USA).

Yield and Nonconverted Monomer Amount Calculation. The calculation of the oligofuranoate yield and the nonconverted monomer amount was done in two different ways depending on the chosen reaction system: solvent system or solvent-free system.

First, for both systems the theoretical oligofuranoate yield was determined based on the applied alcohol concentration (eq 2).

$$\text{mol of applied alcohol} \times \text{g/mol of repeating unit} = \text{theoretical yield [g]} \quad (2)$$

The molecular weight of the poly(butylene) furanoate repeating unit is 210.18 and 264.27 g/mol for the poly(methoxycyclohexyl) furanoate repeating unit.

The second step now differs according to the used system. In general, oligofuranoates produced in the solvent system were precipitated, and this way nonconverted monomers were removed from the product. Therefore, calculation of the nonconverted monomer amount is not possible, and product yield can be calculated by eq 3.

Solvent System.

$$\frac{\text{dried oligofuranoate product [g]}}{\text{theoretical yield [g]}} \times 100 = \text{yield \%} \quad (3)$$

Solvent-Free System. The solvent-free system, in contrast, includes no precipitation step but an evaporation of chloroform. Here, the nonconverted monomers are not removed during the precipitation step and remain in the oligofuranoate product. Therefore, yield calculation of oligofuranoates produced via the solvent-free system includes an additional step: calculation of oligofuranoate product and calculation of nonconverted monomer percentage. This was done using the data from GPC. The peak areas of GPC curves from the oligofuranoate product and the nonconverted monomers were determined using MestReNova software (version: 6.0.2-5475). This way, the percentage of the oligofuranoate product and monomers within the total product solution was calculated.

$$\text{peak area alcohol} + \text{peak area ester} + \text{peak area product} = \text{total product peak area} \quad (4)$$

$$\frac{\text{peak area alcohol}}{\text{total product peak area}} = \text{nonconverted alcohol \%} \quad (5)$$

$$\frac{\text{peak area ester}}{\text{total product peak area}} = \text{nonconverted ester \%} \quad (6)$$

$$\frac{\text{peak area product}}{\text{total product peak area}} = \text{product \%} \quad (7)$$

The oligofuranoate product percentage was then used to calculate the grams of the oligofuranoate product from the grams of total product solution.

$$\frac{\text{product \%}}{100} \times \text{total product solution [g]} = \text{oligofuranoate product [g]} \quad (8)$$

The amount of oligofuranoate product (oligofuranoate product [g]) was then used for yield calculation via eq 9.

$$\frac{\text{oligofuranoate product [g]}}{\text{theoretical yield [g]}} \times 100 = \text{yield \%} \quad (9)$$

RESULTS AND DISCUSSION

The polycondensation (Figure 1A) of dimethyl furan-2,5-dicarboxylate (DMFDCA), as a furan and diethylene gycol (DEG), as a diol via the procedure in Figure 1B has been previously reported by us.[62] While this polymerization proceeds readily, the products do not show OH/OH end groups (not α,ω-telechelic diols), as can be observed in the NMR spectra of Figure 2; an Ester/Ester end group majority becomes obvious.

To overcome this drawback and to generate DEG oligofuranoates with an OH/OH end group majority, different monomer ratios for polycondensation were applied. Instead of equal amounts of ester (DMFDCA) and diol (DEG), less diol (ester/diol: 2:1) and more diol (ester/diol: 2:3) was used. All other parameters shown in Figure 1B were maintained. Additionally, DEG oligofuranoate precipitation in *n*-pentane was tested instead of *n*-hexane, as *n*-pentane is the more commonly used solvent in industrial polyurethane processing and would therefore reduce subsequent reprocessing of the DEG oligofuranoates.

The molecular weights of the DEG oligofuranoates synthesized with monomer ratios of 2:1 (Exp_3) and 2:3 (Exp_4), as well the DEG oligofuranoate synthesized with the 2:2 ratio and precipitated in *n*-pentane (Exp_2_2), are significantly reduced compared to the DEG oligofuranoate successfully reproduced from the literature (Exp_2) (Table 1). These low molecular weight oligofuranoates are very sticky, and even several rounds of precipitation did not result in an improved recovery. Therefore, it was nearly impossible to analyze and characterize these oligomers in an appropriate way

DOI: 10.1021/acssuschemeng.9b05874
ACS Sustainable Chem. Eng. 2020, 8, 1068−1086

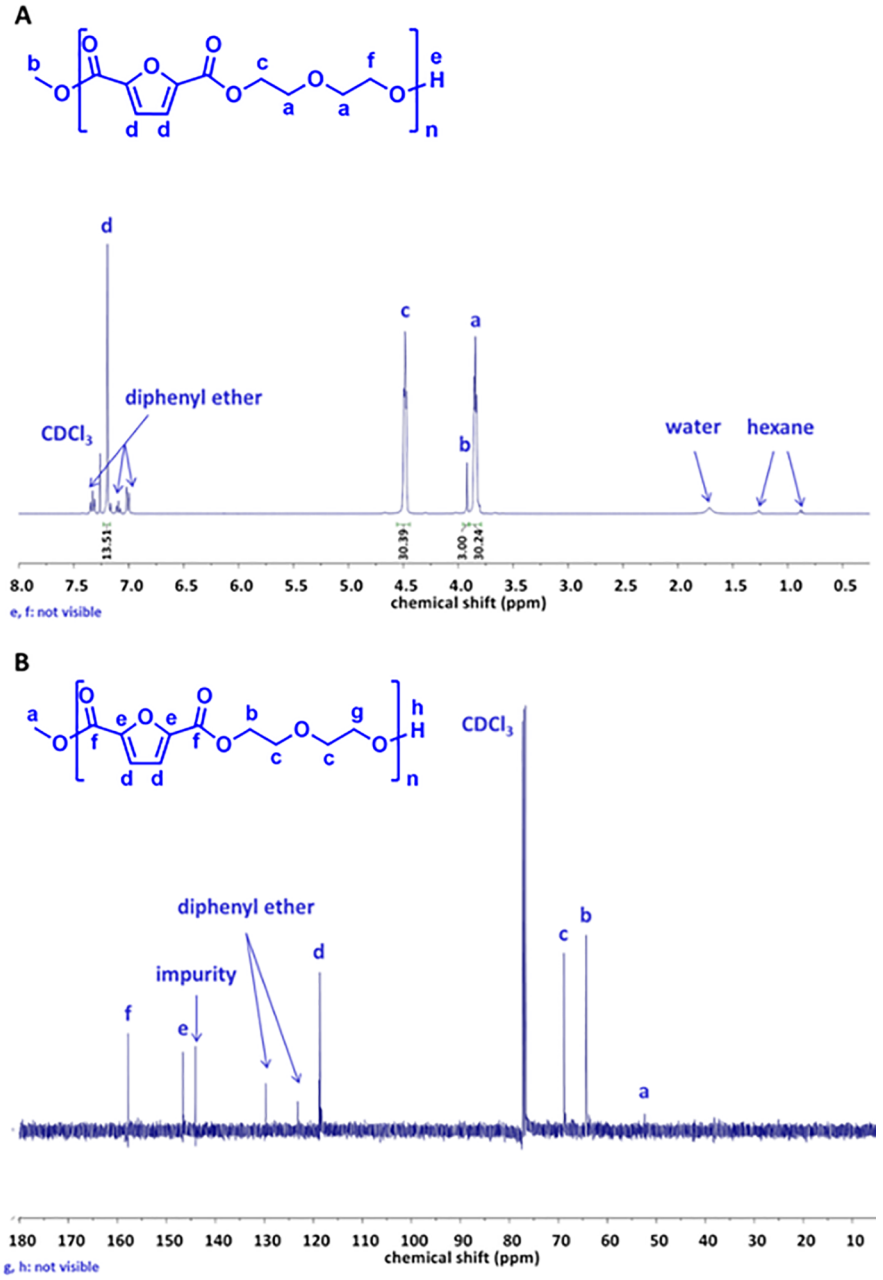

Figure 2. (A) ^{1}H NMR spectrum of poly(diethylene glycol furanoate). Peak integrals showing the corresponding number of protons are indicated, and peaks are labeled with letters for structural assignment. Identified impurities and nonidentified impurities are labeled. (B) ^{13}C NMR spectrum of poly(diethylene glycol furanoate). Peaks are labeled with letters for structural assignment. Identified impurities and nonidentified impurities are labeled.

without losing a large amount of material, and two alternative diols for polycondensation with DMFDCA were studied: 1,4-butanediol (1,4-BDO) and 1,4-cyclohexanedimethanol (1,4-CHDM) (cis/trans mixture).[83]

The polycondesation using these diols will lead to poly(butylene)furanoate, in the following referred to as 1,4-BDO oligofuranoate and poly(methoxycyclohexyl)furanoate, called 1,4-CHDM oligofuranoate (Figure 3A).

For each of the different polycondensations, a blank reaction without immobilized CalB was performed in parallel to exclude oligofuranoate synthesis without enzyme. All polycondensations without CalB did not result in any kind of oligofuranoate synthesis (data not shown). Successful oligofuranoate synthesis was verified by ^{1}H NMR measurement, and the molecular weight was determined by ^{1}H NMR measurement and gel permeation chromatography (GPC). Thermal properties like evaporation, decomposition, melting, and crystallizing behavior were analyzed by thermal gravimetric analysis (TGA) and differential scanning calorimetry (DSC). The final microstructure analysis regarding the OH/OH end group majority was performed by electrospray ionization high resolution mass spectrometry (ESI-HRMS).

Polycondensations with DMFDCA and 1,4-BDO and 1,4-CHDM were performed with one major aim: to identify a suitable diol for generating oligofuranoates that are easy to characterize and show a majority of OH/OH end groups. The

DOI: 10.1021/acssuschemeng.9b05874
ACS Sustainable Chem. Eng. 2020, 8, 1068−1086

Table 1. Summary of Polycondensations of Dimethyl Furan-2,5-dicarboxylate with Diethylene Glycol[a]

			GPC			
exp.	ratio	precipitation	$\overline{M_n}$	$\overline{M_w}$	Đ	yield %
2_2	2:2	*n*-pentane	695	949	1.37	–
3	2:1		983	1414	1.44	–
2	2:2	*n*-hexane	2648	8173	3.09	58
4	2:3		326	431	1.32	–

[a]Experimental number, used monomer ratio, precipitation solvent, number-average ($\overline{M_n}$) and weight-average ($\overline{M_w}$) molecular weights (g/mol) determined via gel permeation chromatography (GPC), calculated dispersity, and yield of generated diethylene glycol oligofuranoates are shown.

different properties of the two oligofuranoates will not be discussed in detail, but striking differences will be highlighted. In general, polycondensation with both diols in different ratios showed successful oligofuranoate synthesis as indicated by the chemical shift in the ^{1}H NMR spectra related to ester bond formation (1,4-BDO, Figure 4A red box and asterisk; 1,4-CHDM, Figure 5A red box and asterisk). The 1,4-CHDM oligofuranoates show nearly similar molecular weights independent from the applied monomer ratio (Figure 5B, molecular weight analysis). The 1,4-BDO oligofuranoates show differences in molecular weight based on the diol amount used. When using less or more diol (2:1 or 2:3), the molecular weight is drastically decreased to more than a half, compared to the molecular weight of the 1,4-BDO oligofuranoate achieved with a 2:2 ratio (Figure 4B, molecular weight analysis). The higher molecular weight oligofuranoates show higher melting temperatures and are more stable as proven by decomposition rates (1,4-BDO, Figure 4B, thermal analysis Exp_5; 1,4-CHDM, Figure 5B, thermal analysis Exp_8–10). This can be explained by the structural differences of the used diols. The aliphatic 1,4-BDO is more flexible than the cyclic 1,4-CHDM. This may negatively influence the propagation of the polycondensation of poly(butylene) furanoate leading to an early termination and therefore to a decrease in molecular weights, resulting in lower melting temperatures. No glass transition temperature could be determined for both oligofuranoates (Figure 4B and Figure 5B, thermal analysis). The reason could be imperfect or different crystal forms combined with amorphous areas of the oligofuranoates that prevent a consistent transition into the viscous phase. This assumption is underlined by the detection of two or more melting temperatures for 1,4-BDO and 1,4-CHDM oligofuranoates. Such bimodal or trimodal melting points are known for oligomer heterogeneity. More important than the molecular weight of the thermal properties of the oligofuranoates is the end-group majority generated. By comparison of the results from the microstructure analysis of the 1,4-BDO and the 1,4-CHDM oligofuranoates (Figure 4B and Figure 5B, microstructure analysis), a great difference between the two oligofuranoates could be observed. Where the 1,4-BDO oligofuranoates predominantly show a large variety of end groups (Figure 4B, microstructure analysis), 1,4-CHDM oligofuranoates predominantly show Ester/Ester and Ester/OH end groups (Figure 5B, microstructure analysis). Only one of the oligofuranoates showed the desired majority of OH/OH end groups: the 1,4-CHDM oligofuranoate synthesized with a 2:3 monomer ratio (Figure 5B, microstructure analysis Exp_10). This was already indicated by the ^{1}H NMR spectrum (Figure 5A, 2:3) in which the peaks from chemical shifts of the 1,4-CHDM end groups can be clearly seen (blue box and astersisk) compared to a decrease in the ester end group of the DMFDCA (magenta box and astersisk). This explains the high molecular weight calculation of this 1,4-CHDM oligofuranoate via ^{1}H NMR measurement (Figure 5B, molecular weight analysis Exp_10, astersisk) because the protons from the methyl ester end group of the DMFDCA were generally used as the reference end group for molecular weight determination. If this end group is now proportionally low compared to the diol end group, the calculated molecular weight gets relatively high.

Although the yield of the synthesized oligofuranoate is quite low so far, about 20%, 1,4-CHDM in the 2:3 monomer ratio with the established experimental set up was chosen for subsequent optimization strategies in terms of oligofuranoate recovery and oligofuranoate synthesis time and temperature, as well as the amount of enzymatic catalyst necessary for the highest oligofuranoate yield.

The established and so far used experimental set up for polycondensation of DMFDCA and 1,4-CHDM includes

A

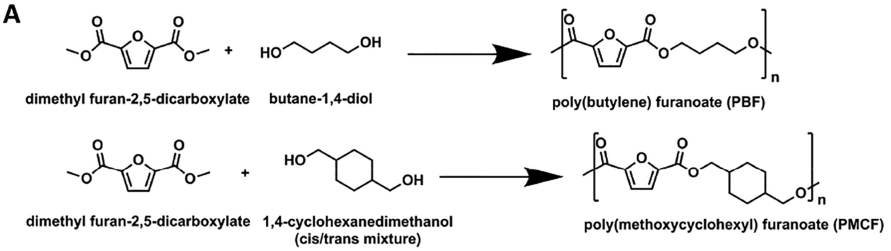

B

parameters	1	2	3
Monomer amount	30 % of total reaction volume		
Monomer ratio	2:1	2:2	2:3
Enzyme amount/Lewatit beads amount	25 wt%		
Solvent	diphenyl ether		
Solvent amount	380 wt %		
Temperature	80 °C		
Time	2/72 h		
Surrounding (N_2,vacuum)	N_2/2 mmHg		

Figure 3. (A) Polycondensation of dimethyl furan-2,5-dicarboxylate with 1,4-butanediol and 1,4-cyclohexanedimethanol. (B) Experimental set up of polycondensation.

DOI: 10.1021/acssuschemeng.9b05874
ACS Sustainable Chem. Eng. 2020, 8, 1068–1086

A

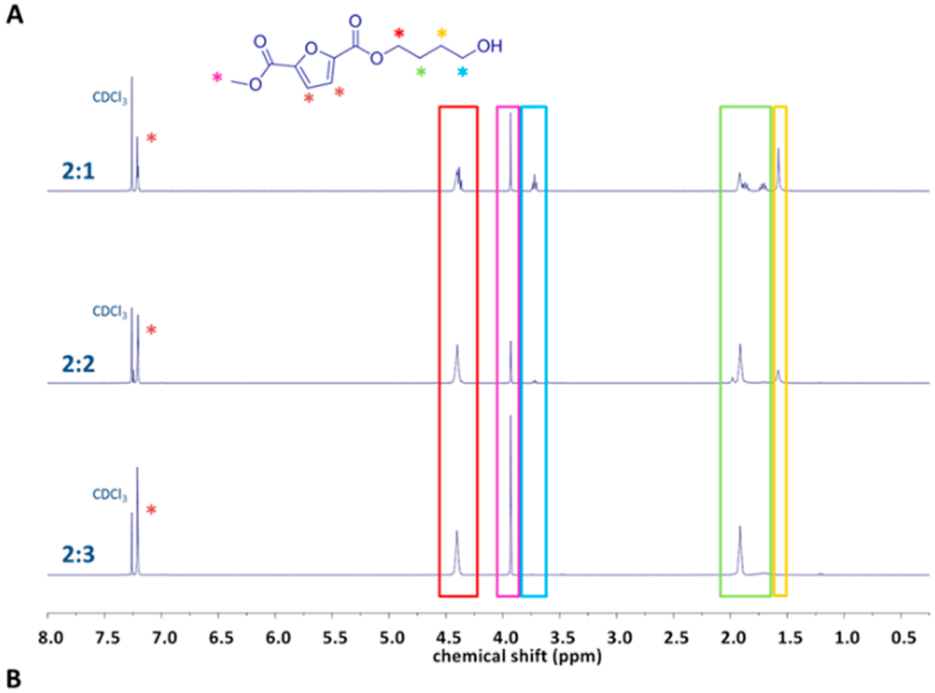

B

Molecular weight analysis / **Microstructure analysis**

Exp.	Ratio	Yield %	^{1}H-NMR $\overline{M_n}$	GPC $\overline{M_n}$	GPC $\overline{M_w}$	Đ	End groups 1st	2nd	3rd
6	2:1	19	420	565	610	1.08	Ester/Ester	Ester/OH	OH/OH
5	2:2	15	631	1826	2130	1.16	Aldehyde/Ester	Ester/Ester	Ester/OH
7	2:3	86	210	772	1035	1.34	Ester/Ester	OH/OH	Ester/Acid

Thermal analysis

Exp.	Ratio	$T_{d\text{-}5\%}$ [°C]	$T_{d\text{-}max}$ [°C]	T_g [°C]	T_m [°C]	T_c [°C]	T_{cc} [°C]
6	2:1	203	261/384	-	70	-	46
5	2:2	287	292/387	-	132/148	65	-
7	2:3	240	277/384	-	100/109/130	117	69

Figure 4. Results of polycondensation of dimethyl furan-2,5-dicarboxylate with 1,4-butanediol. (A) Comparison of ^{1}H NMR spectra of poly(butylene) furanoates generated with different monomer ratios. Peaks are indicated with boxes colored to the corresponding asterisk for structural assignment. (B) Poly(butylene) furanoates characterization. Molecular weight analysis: Experimental number, used monomer ratio, calculated yield, number-average ($\overline{M_n}$) calculated via ^{1}H NMR and GPC, weight-average ($\overline{M_w}$) molecular weight (g/mol) determined via GPC, and calculated dispersity are shown. Microstructure analysis: End groups identified via ESI-HRMS are classified according to the HRMS peak intensity of the corresponding measured molecular weight for this end group species. Thermal analysis: Experimental number, used monomer ratio, temperature of 5% weight loss ($T_{d\text{-}5\%}$), highest weight loss rate% per temperature °C, indicating the maximum rate of decomposition ($T_{d\text{-}max}$), glass transition temperature (T_g), melting temperature (T_m), crystallization (T_c), and cold crystallization (T_{cc}) are shown.

diphenyl ether as the polycondensation solvent and a subsequent precipitation of the generated 1,4-CHDM oligofuranoate in diethyl ether for its recovery and purification. This oligofuranoate recovery by precipitation includes a high amount of precipitation solvent and an overnight step of precipitation at −20 °C. These are conditions that would render an industrial large-scale oligofuranoate production too time and cost intensive. Therefore, the recovery of the oligofuranoate by precipitation was substituted with a simple evaporation step of the oligomer-dissolving solvent chloroform. This simplifies the reprocessing of the oligofuranoate. It can, however, complicate its analysis and characterization because the nonconverted monomers DMFDCA and 1,4-CHDM will not be removed from the oligomer. Nevertheless, polycondensation was peformed with DMFDCA and 1,4-CHDM in a 2:3 ratio under the established experimental parameters. After dissolving the oligofuranoate in chloroform and filtering of the immobilized CalB, the chloroform was evaporated, and the oligomer was

DOI: 10.1021/acssuschemeng.9b05874
ACS Sustainable Chem. Eng. 2020, 8, 1068−1086

A

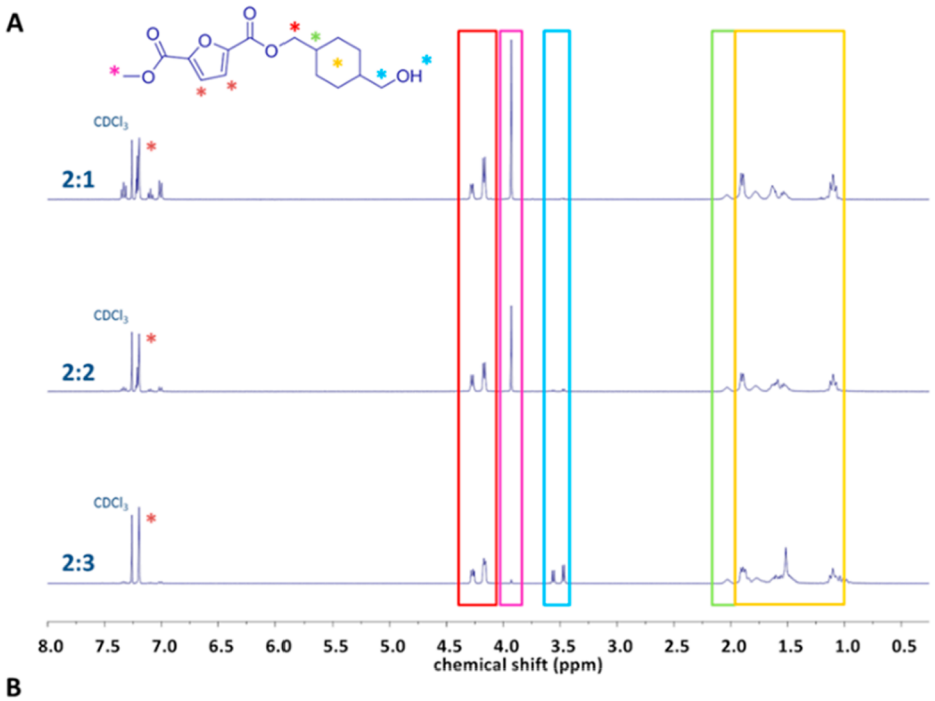

B

Molecular weight analysis / **Microstructure analysis**

Exp.	Ratio	Yield %	^{1}H-NMR $\overline{M_n}$	GPC $\overline{M_n}$	GPC $\overline{M_w}$	Đ	End groups 1st	2nd	3rd
9	2:1	53	370	1196	1593	1.33	Ester/Ester	Ester/OH	Aldehyde/Ester
8	2:2	26	634	1605	1957	1.22	Ester/Ester	Ester/OH	-
10	2:3	20	19133*	1267	1501	1.18	OH/OH	-	-

Thermal analysis

Exp.	Ratio	$T_{d\text{-}5\%}$ [°C]	$T_{d\text{-}max}$ [°C]	T_g [°C]	T_m [°C]	T_c [°C]	T_{cc} [°C]
9	2:1	304	330/398	-	123/203	80/133/183	-
8	2:2	319	335/400	-	142/234	153/165	-
10	2:3	287	307/403	-	140/170/240 /255	182	-

Figure 5. Results of polycondensation of dimethyl furan-2,5-dicarboxylate with 1,4-cyclohexanedimethanol. (A) Comparison of ^{1}H NMR spectra of poly(methoxycyclohexyl) furanoates generated with different monomer ratios. Peaks are indicated with boxes colored to the corresponding asterisk for structural assignment. (B) Poly(methoxycylohexyl) furanoates characterization. Molecular weight analysis: Experimental number, used monomer ratio, calculated yield, number-average ($\overline{M_n}$) calculated via ^{1}H NMR and GPC, weight-average ($\overline{M_w}$) molecular weight (g/mol) determined via GPC, and calculated dispersity are shown. Microstructure analysis: End groups identified via ESI-HRMS are classified according to the HRMS peak intensity of the corresponding measured molecular weight for this end group species. Thermal analysis: Experimental number, used monomer ratio, temperature of 5% weight loss ($T_{d\text{-}5\%}$), highest weight loss rate% per temperature °C, indicating the maximum rate of decomposition ($T_{d\text{-}max}$), glass transition temperature (T_g), melting temperature (T_m), crystallization (T_c), and cold crystallization (T_{cc}) are shown.

analyzed by ^{1}H NMR spectroscopy. The ^{1}H NMR spectrum showed a large remaining amount of the diphenyl ether solvent that could not be removed from the oligofuranoate sufficiently. Even several rounds of redissolving in chloroform and evaporation could not solve this problem (data not shown). Since the diphenyl ether has to be removed completely from the oligofuranoate otherwise impeding the oligomer analysis, it was decided to try a solvent-free/bulk polycondensation system. This way the presence and subsequent removal of high-boiling diphenyl ether was avoided completely. The common solvent system with subsequent oligofuranoate precipitation was performed according to the usual experimental set up in parallel to the solvent-free system without the polycondensation solvent diphenyl ether and subsequent evaporation of the oligomer-dissolving solvent chloroform. The synthesized oligofuranoates

DOI: 10.1021/acssuschemeng.9b05874
ACS Sustainable Chem. Eng. 2020, 8, 1068−1086

A

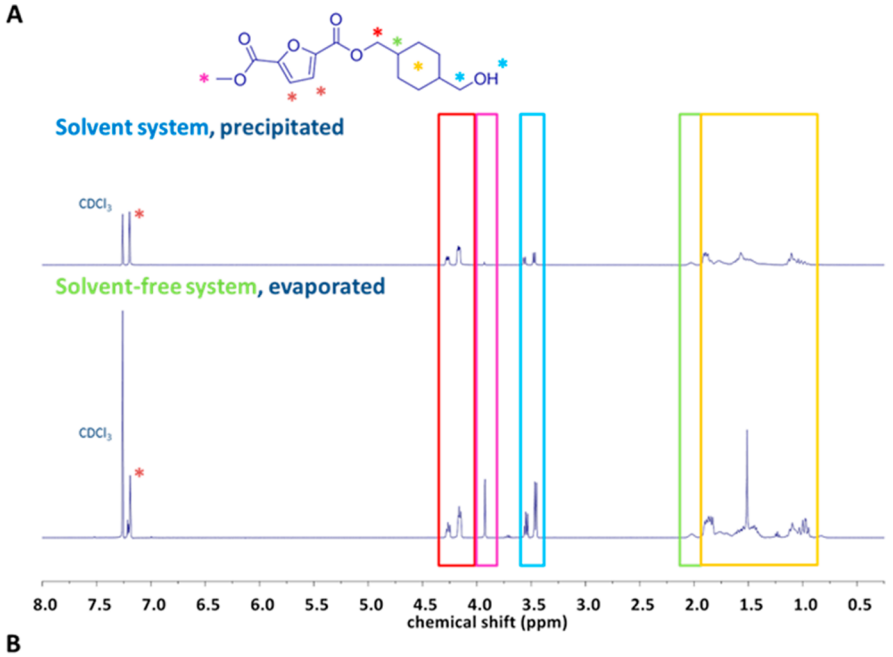

B

Molecular weight analysis

Exp.	Solvent	Yield %	^{1}H-NMR $\overline{M_n}$	GPC $\overline{M_n}$	GPC $\overline{M_w}$	Đ
13	yes	19	524	1227	1428	1.16
16	no	61	270*	752	965	1.3

Figure 6. Molecular weight analysis of the poly(methoxycyclohexyl) furanoates synthesized in solvent and solvent-free systems. (A) Comparison of ^{1}H NMR spectra of poly(methoxycyclohexyl) furanoates generated in the two systems. Peaks are indicated with boxes colored to the corresponding asterisk for structural assignment. (B) Poly(methoxycyclohexyl) furanoate molecular weight analysis. The experimental number, the used monomer ratio, the calculated yield, the number-average ($\overline{M_n}$) calculated via ^{1}H NMR and GPC and weight-average ($\overline{M_w}$) molecular weight (g/mol) determined via GPC and the calculated dispersity are shown.

were analyzed and characterized by the previously mentioned methods.

^{1}H NMR measurements of both 1,4-CHDM oligofuranoates confirm oligomerization (Figure 6A). This means that polycondensation of DMFDCA and 1,4-CDHM is possible in a solvent free/bulk system. The different intensity of the peak from the protons of the methyl group of the DMFDCA ester (Figure 6A, magenta box and asterisk) is quite striking. The peak intensity of the 1,4-CHDM (Figure 6A, yellow box and asterisk) is significantly higher within the spectra of the oligofuranoate synthesized in the solvent-free system. This indicates the amount of nonconverted monomers that were not removed from the oligofuranoate and complicates the oligofuranoate characterization. As shown in Figure 6B Exp_16, the molecular weight calculated via ^{1}H NMR measurement is marked with an asterisk because the spectra of the remaining monomers overlap with the spectra of the oligofuranoate and cannot be differentiated. They therefore disturb molecular weight determination via ^{1}H NMR spectroscopy. The molecular weights for the solvent-free generated oligofuranoate determined by GPC are influenced by the remaining monomers, too.

The higher amount of low molecular weight species is leading to a nearly 2-fold decrease in molecular weight compared to the oligofuranoate synthesized in the solvent system with selective precipitation (Figure 6B Exp_13). The amount of nonconverted monomers within the solvent-free synthesis was determined via GPC and subsequent calculation (Figure 7A). In the oligofuranoate synthesized with the solvent system (Figure 7A blue line), the amount of unreacted monomers was not recorded. The solvent-free generated oligofuranoate showed a total nonconverted monomer amount of about 17% (Figure 7A, green line and table) and an oligofuranoate amount of 83%. With these amounts of nonconverted monomers, the oligofuranoate yield is 61% (Figure 6B Exp_16). Monomer evaporation is nicely shown during thermal gravimetric analysis when the solvent-free generated oligofuranoate (Figure 7B, green line indicated with red arrows) is compared to the oligofuranoate of the solvent system (Figure 7B, blue line indicated with red arrows). Both 1,4-CHDM oligomers show similar decomposition temperatures of about 230 °C for $T_{d\text{-}5\%}$ and 290/400 °C for $T_{d\text{-}max}$. This means that both syntheses protocols are able to yield similar 1,4-CHDM oligofuranoates that increases the thermal stability of DMFDCA by about 100 °C. Thermal degradation of polyester compounds is usually a single stage process. This stage mainly involves nonradical decomposition, radical alkyl-oxygen homolysis, and radical acryl-oxygen homolysis. The result is a precursor to the formation of an intramolecular transesterification, which undergoes ester pyrolysis, and unzipping depolymerization random chain

DOI: 10.1021/acssuschemeng.9b05874
ACS Sustainable Chem. Eng. 2020, 8, 1068−1086

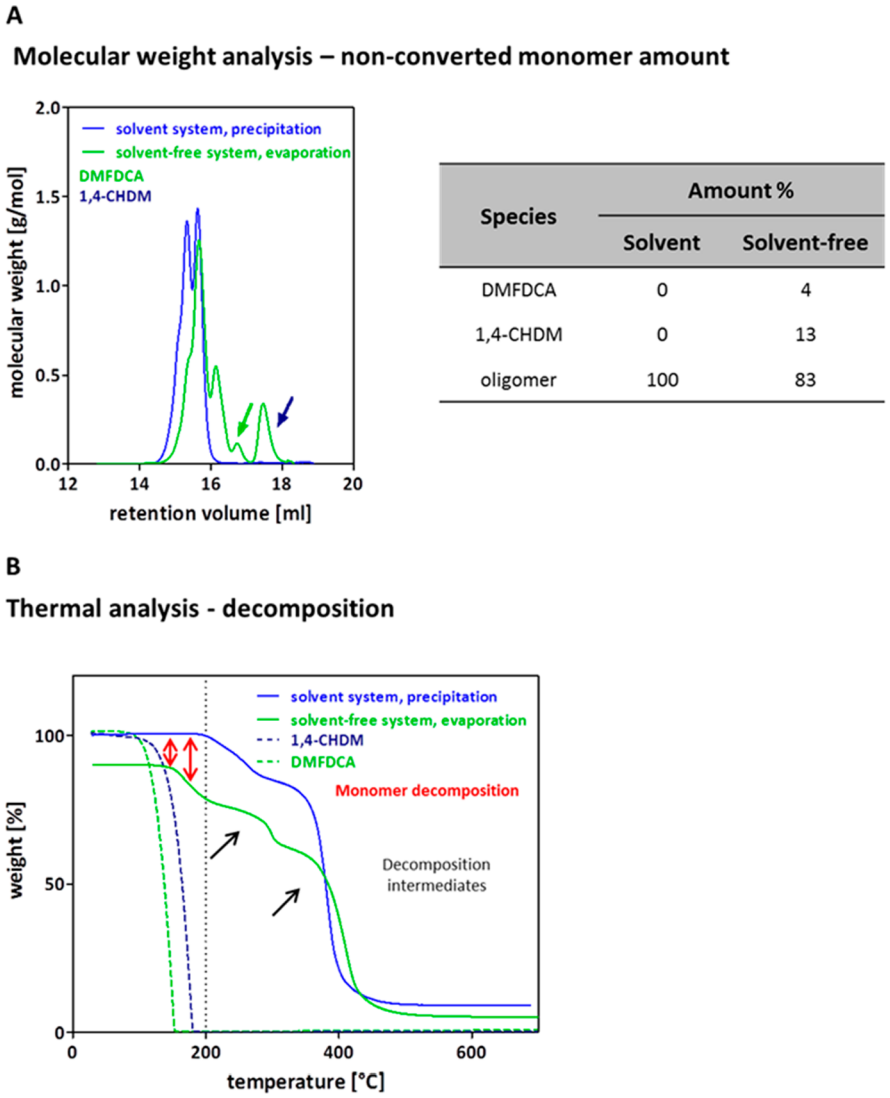

Species	Amount %	
	Solvent	Solvent-free
DMFDCA	0	4
1,4-CHDM	0	13
oligomer	100	83

Figure 7. Nonconverted monomer amount within the poly(methoxycyclohexyl) furanoates synthesized in solvent and solvent-free systems. (A) Monomer and oligofuranoate calculation within the poly(methoxycyclohexyl) furanoates. The GPC elugram is shown, and peaks of nonconverted DMFDCA and 1,4-CHDM are indicated. Calculated nonconverted monomer and oligofuranoate amounts are shown. (B) Thermal decomposition of poly(methoxycyclohexyl) furanoates. The monomer decomposition as well as the occurring decomposition intermediates are indicated.

scission.[84] This process explains the observed molecular weight dependence of thermal stability of our compounds.

The molecular weight determination and oligofuranoate decomposition (Figure 8) microstructure analysis proves the impact of the nonconverted monomers on oligofuranoate characterization. Besides the additional majority of Ester/OH end groups in oligofuranoates from the solvent-free protocol (Table 2 Exp_16) compared to the solely dominant OH/OH end group of oligomers synthesized via the solvent protocol (Table 2 Exp_13), ESI-HRMS results show a higher distribution and variety of oligomer species when production is solvent-free. Nevertheless, also the solvent-free system provides an OH/OH end group majority.

The melting and crystallinity behavior of both 1,4-CHDM oligofuranoates was determined by DSC measurements. Additionally, the melting of monomers DMFDCA and 1,4-CHDM was analyzed to allow differentiation between monomer and oligofuranoate melting within the 1,4-CHDM oligofuranoate synthesized with the solvent-free system. The monomers are melting at 57 °C (1,4-CHDM) and at 111 °C (DMFDCA) (Figure 8, first heating blue and green dotted line), and this melting is also visible during solvent-free generated oligofuranoate melting indicated in one broad peak between 50 and 111 °C (Figure 8, first heating green line).

Based on this, a sufficient separation and assignment of the several peaks within the melting of the solvent-free generated oligofuranoate is possible. The oligofuranoate generated with the solvent system (Figure 8, first heating blue line) is melting at 169/180 °C. The melting of the solvent-free produced oligofuranoate is observed already at 130−150 °C (Figure 8, first heating green line). The reason for this is the monomer content that results to a 2-fold lower molecular weight of the solvent-free produced oligofuranoate. Nevertheless, both oligofuranoates show the already previously observed bimodal melting behavior based on the mixture of semicrystalline and armorphous oligomeric structures. Like the melting temperature, also the crystallization temperature of the solvent-free produced oligofuranoate is shifted to lower temperatures related to the similar reasons.

DOI: 10.1021/acssuschemeng.9b05874
ACS Sustainable Chem. Eng. 2020, 8, 1068−1086

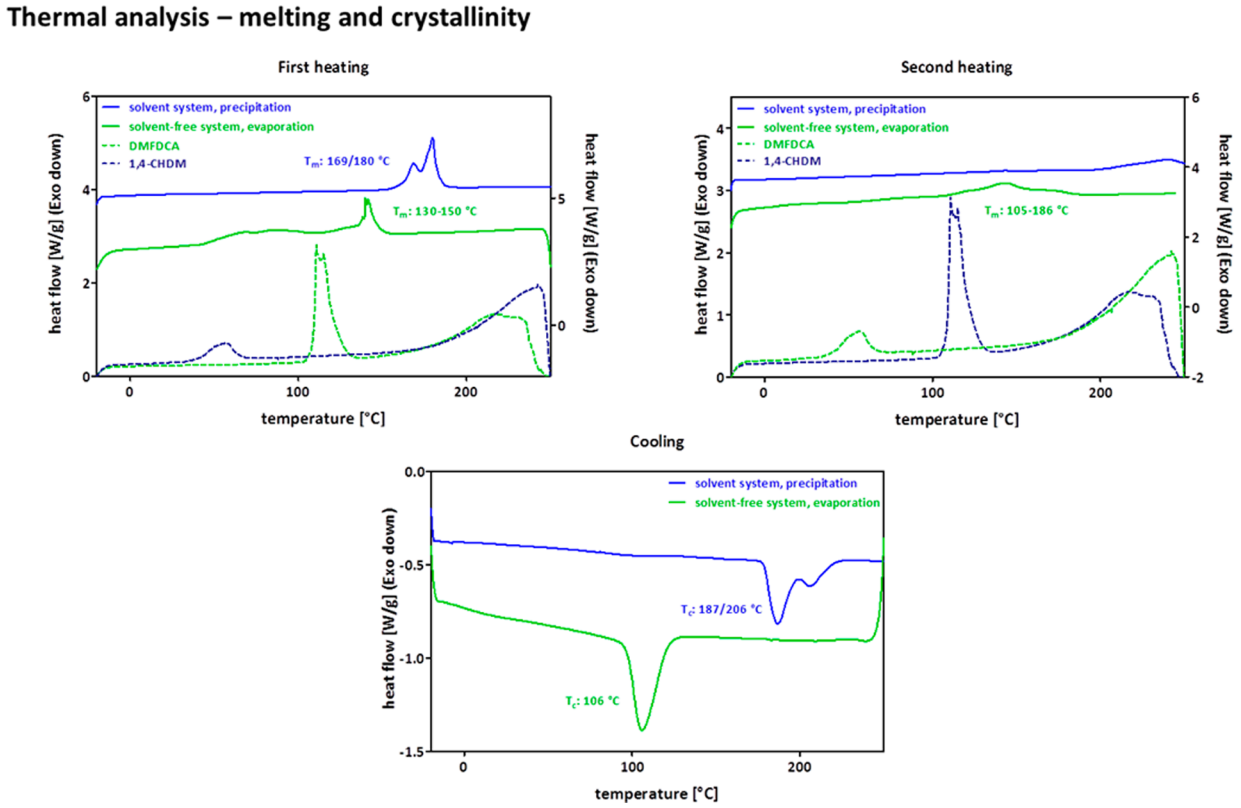

Figure 8. Melting and crystallizing behavior of poly(methoxycyclohexyl) furanoates synthesized in solvent and solvent-free systems. The first heating step, cooling step,and second heating from DSC measurement of the oligofuranoates and monomers DMFDCA and 1,4-CHDM are shown. The determined melting temperatures (T_m) and crystallization temperatures (T_c) are indicated.

Table 2. Microstructure Analysis of Poly(methoxycyclohexyl) Furanoates Synthesized in Solvent and Solvent-Free Systems[a]

		end groups		
exp.	solvent	first	second	third
13	yes	OH/OH	OH/OH	–
16	no	OH/OH	Ester/OH	Ester/OH

[a]End groups identified via ESI-HRMS are classified according to the HRMS peak intensity of the corresponding measured molecular weight for this end-group species.

It can be concluded that it is possible to generate 1,4-CHDM oligofuranoate in solvent and solvent-free systems. Residual monomers that are not removed by precipitation change the average molecular weight and thermal properties of the oligomer. An experiment in which the solvent-free synthesized oligofuranoate was precipitated could prove similar properties of this oligofuranoate compared to the one generated in the solvent system. Therefore, the solvent-free system will be used in upcoming optimization approaches targeting polycondensation time and temperature, enzyme amount applied, bypassing high solvent amounts, and time expenditure for oligofuranoate recovery by precipitation.

Solvent-free polycondensation was performed according to the established set up for three different polycondensation times of 24, 48, and 72 h. Due to the overlapping ^{1}H NMR spectra of the monomers and oligofuranoate, the molecular weight will be no longer determined by ^{1}H NMR measurement. The determination of the melting temperature will be performed based on the second heating during DSC measurement because of measurement inconsistencies during the first heating related to monomer and low molecular weight species melting here.

Table 3. Results of Polycondensation of Dimethyl Furan-2,5-dicarboxylate with 1,4-Cyclohexanedimethanol[a]

			molecular weight analysis				microstructure analysis		
			^{1}H NMR	GPC			end groups		
exp.	time [h]	yield %	$\overline{M_n}$	$\overline{M_n}$	$\overline{M_w}$	Đ	first	second	third
14	24	92	n.d.	601	788	1.3	Ester/OH	OH/OH	Ester/OH
15	48	82	n.d.	684	890	1.3	OH/OH	Ester/OH	Ester/OH
16	72	61	n.d.	752	965	1.3	OH/OH	Ester/OH	Ester/OH

[a]Molecular Weight Analysis: The experimental number, the used monomer ratio, the calculated yield, the number average ($\overline{M_n}$) calculated via ^{1}H NMR and GPC and weight average ($\overline{M_w}$) molecular weight (g/mol) determined via GPC and the calculated dispersity are shown. Microstructure analysis: End groups identified via ESI-HRMS are classified according to the HRMS peak intensity of the corresponding measured molecular weight for this end group species.

DOI: 10.1021/acssuschemeng.9b05874
ACS Sustainable Chem. Eng. 2020, 8, 1068−1086

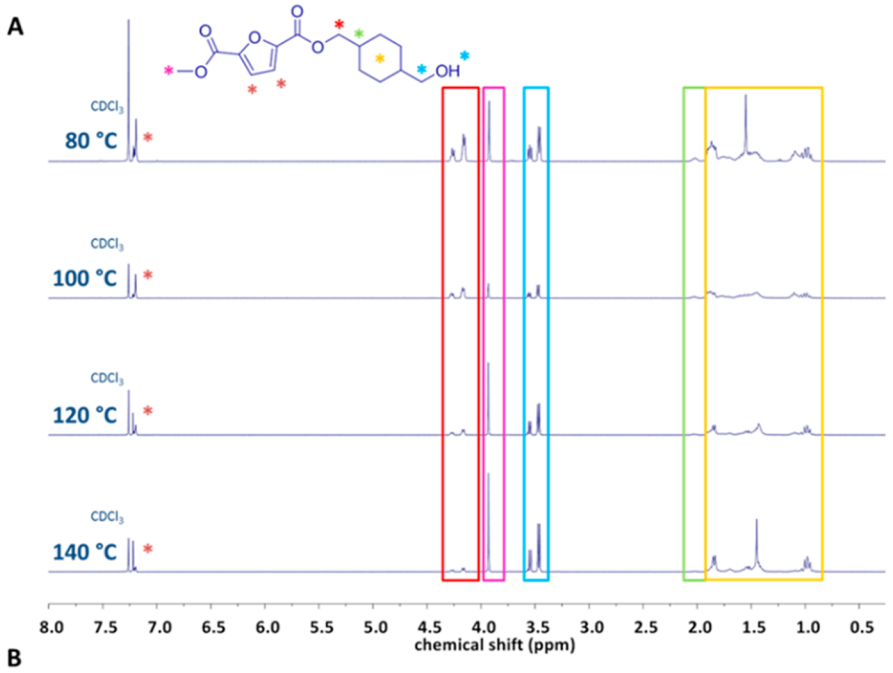

B

Molecular weight analysis – non-converted monomer amount

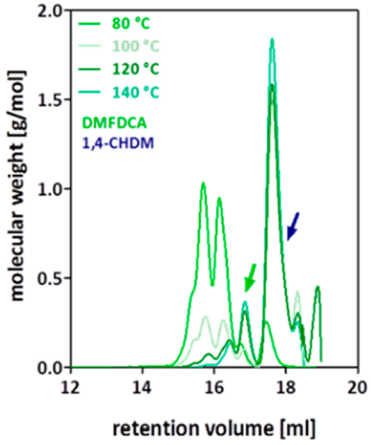

Species	Amount %			
	80 °C	100 °C	120 °C	140 °C
DMFDCA	4	3	11	12
1,4-CHDM	9	69	78	83
oligomer	87	28	11	5

Figure 9. Results of polycondensation of dimethyl furan-2,5-dicarboxylate with 1,4-cyclohexanedimethanol. A - Comparison of ^{1}H NMR spectra of poly (methoxycyclohexyl) furanoates generated at different temperatures. Peaks are indicated with boxes colored to the corresponding asterisk for structural assignment. B - Monomer and oligofuranoate calculation within the poly (methoxycyclohexyl) furanoates. The GPC elugram is shown and peaks of nonconverted DMFDCA and 1,4-CHDM are indicated. Calculated nonconverted monomer and oligofuranoate amounts are shown.

The resulting oligofuranoates were analyzed and characterized by the previously mentioned methods. 1,4-CHDM oligofuranoates are successfully synthesized in the solvent-free system with 24, 48, or 72 h high vacuum polycondensation times. They show similar properties regarding their molecular weight, the residual monomer amount and their thermal behavior. Differences that were crucial for identifying the most convenient polycondensation time are the 1,4-CHDM oligofuranoate yield and the end group majority (Table 3). The oligofuranoate yield is 92% after 24 h of high-vacuum polycondensation. With increasing polycondensation time the oligofuranoate yield decreases. This can be explained by product inhibition of the enzyme. The end groups of the different oligofuranoate species are classified according to the HRMS peak intensity of the corresponding molecular weight for this end group species. All of these intensities are nearly similar distributed (Table 3). All three oligofuranoates show species with OH/OH end groups. Therefore, it was decided to choose 24 h of polycondensation time that yielded 92% and ester/OH and OH/OH end group majority.

The enzymatically synthesized 1,4-CHDM oligofuranoates have a low viscosity and therefore the lipase-catalyzed polycondensation was repeated at higher temperatures to synthesize 1,4-CHDM oligofuranoates with increased viscosity. Although this seems in quite contrast to the initial aim of this project, it has been shown that the chosen model furan dimethyl furan-2,5-dicarboxylate is stable until a polycondensation temperature of 140 °C.[74] Oligofuranoates synthesized at this elevated temperature show a higher molecular weight compared to those at 80 °C. This could positively influence the oligomer viscosity.

DOI: 10.1021/acssuschemeng.9b05874
ACS Sustainable Chem. Eng. 2020, 8, 1068−1086

Table 4. Characterization of Poly(methoxycyclohexyl) Furanoates[a]

molecular weight analysis							microstructure analysis		
			^{1}H NMR	GPC			end groups		
exp.	temp. [°C]	yield %	$\overline{M_n}$	$\overline{M_n}$	$\overline{M_w}$	Đ	first	second	third
14	80	92	n.d.	601	788	1.3	Ester/OH	OH/OH	Ester/OH
19	100	19	n.d.	1103	1291	1.2	OH/OH	Ester/OH	Ester/OH
20	120	10	n.d.	948	1107	1.2	Ester/OH	Ester/OH	OH/OH
21	140	3	n.d.	874	966	1.1	Ester/OH	OH/OH	Ester/Ester

Thermal analysis							
exp.	temp. [°C]	$T_{d\text{-}5\%}$ [°C]	$T_{d\text{-}max}$ [°C]	T_g [°C]	T_m [°C]	T_c [°C]	T_{cc} [°C]
14	80	170	309/408	–	111–190	106/127	–
19	100	226	282/396	–	112–211	121	–
20	120	167	231/396	–	–	–	–
21	140	145	227/386	–	–	–	–

[a]Molecular weight analysis: The experimental number, the used monomer ratio, the calculated yield, the number-average ($\overline{M_n}$) calculated via ^{1}H NMR and GPC and weight-average ($\overline{M_w}$) molecular weight (g/mol) determined via GPC and the calculated dispersity are shown. Microstructure Analysis: End groups identified via ESI-HRMS are classified according to the HRMS peak intensity of the corresponding measured molecular weight for this end-group species. Thermal Analysis: The experimental number, used monomer ratio, temperature of 5% weight loss ($T_{d\text{-}5\%}$), highest weight loss rate% per temperature °C, indicating the maximum rate of decomposition ($T_{d\text{-}max}$), glass transition temperature (T_g), melting temperature (T_m), crystallization (T_c), and cold crystallization (T_{cc}) are shown.

Using the established experimental set up three different increased temperatures, 100 °C, 120 and 140 °C were applied after initial oligomerization at 80 °C for 2 h. As usual, the oligofuranoates were analyzed and characterized by the previously mentioned methods. According to the ^{1}H NMR spectra of the 1,4-CHDM oligofuranotes the amount of oligomer is drastically decreasing with increasing polycondensation temperature (Figure 9A, red boxes). The low amount of polycondensation product and therefore high amounts of nonconverted monomers, up to 80% when oligomerized at 140 °C, are confirmed by thermal gravimetric analysis and gel permeation chromatography (Figure 9B).

The calculated 1,4-CHDM oligofuranoate amount is decreasing from nearly 90% when synthesized at 80 °C to only 5% when the polycondensation temperature was increased to 140 °C (Figure 9B). This of course resulted in an overall low yield of 1,4-CHDM oligofuranoate synthesized at temperatures above 100 °C (Table 4, molecular weight analysis). It has already been shown that CalB-catalyzed oligofuranoate synthesis can yield increasing molecular weights with increased polycondensation temperature.[74] However, there studies were performed in a solvent polycondensation system using diphenyl ether as the reaction solvent. It is possible that in this currently used solvent-free system the immobilized lipase CalB is degraded under increased temperatures due to a lack of stability that might be provided by the diphenyl ether. This in turn leads to a lower oligomerization rates, finally resulting in decreased 1,4-CHDM oligofuranoate yields of 3 to 19% (Table 4, molecular weight analysis Exp_19–21).

As previously described for 1,4-CHDM oligofuranoates from the solvent-free system also here a mixture of Ester/OH and OH/OH end group majority is detected (Table 4, microstructure analysis) and should be sufficient for the later polycondensation.

A determination of the melting crystallization temperatures of the 1,4-CHDM oligofuranoates synthesized at 120 and 140 °C was not possible, due to the fact that these two are mostly consisting of monomers (Table 4, thermal analysis Exp_20 and 21). Oligofuranoates produced at 80 and at 100 °C show similar thermal properties. Evaporation of monomers is starting at about 170 or 200 °C. Melting temperatures range between 111 and 200 °C (Table 4, thermal analysis Exp_14 and 19). These results clearly show that the initially chosen oligomerization temperature of 80 °C is the most suitable one for the oligofuranoate synthesis in the solvent-free system. At temperatures above 100 °C the enzymatic catalyst CalB is not stable without a reaction solvent that is assumed to be protective.

With these optimization strategies, it was possible to reduce the time effort for the enzymatic synthesis of 1,4-CHDM oligofuranoates from around 96 h, including polycondensation and oligofuranoate recovery, to 24 h. This was accomplished by establishing a solvent-free system for synthesis that allows subsequent easy evaporation of the oligomer dissolving solvent. This eliminates overnight precipitation for oligofuranoate recovery. Simultaneously, high yields of 1,4-CHDM oligofuranoates (92% Exp_14) are achieved at low energy costs due to polycondensation at moderate temperatures of 80 °C.

The most cost intensive parameter in this lipase-catalyzed synthesis of furan oligomers, especially regarding a later large-scale production, is the immobilized CalB enzyme catalyst. To reduce these costs, it is interesting to reduce the enzyme amounts used for the polycondensation. In general, 1,4-CHDM oligofuranoates that have been synthesized with 10, 15, and 20 wt % immobilized CalB show similar molecular weight, microstructure, and thermal properties as the previously generated oligofuranoates.

As shown in Figure 10A, oligofuranoates were successfully synthesized with varying biocatalyst amounts. They show similar amounts of nonconverted monomers compared to the 1,4-CHDM oligofuranoate generated with 25 wt % of immobilized CalB (Figure 10B). The highest amount of 1,4-oligofuranoate (85 and 87%) is achieved using 15 and 25 wt % of enzyme. The yield is slightly decreased to 73% and 76% when using 10 and 20 wt % of enzyme. This inconsistency of the relation between enzyme amount and yield is due to nonuniform mixture of the reaction components. This nonuniform miscibility in turn is based on the use of a solvent-free system whose higher viscosity, compared to the solvent based system, hampers a comparable mixing of all components when different experiments are compared. This assumption is confirmed by reproduction of the

DOI: 10.1021/acssuschemeng.9b05874
ACS Sustainable Chem. Eng. 2020, 8, 1068–1086

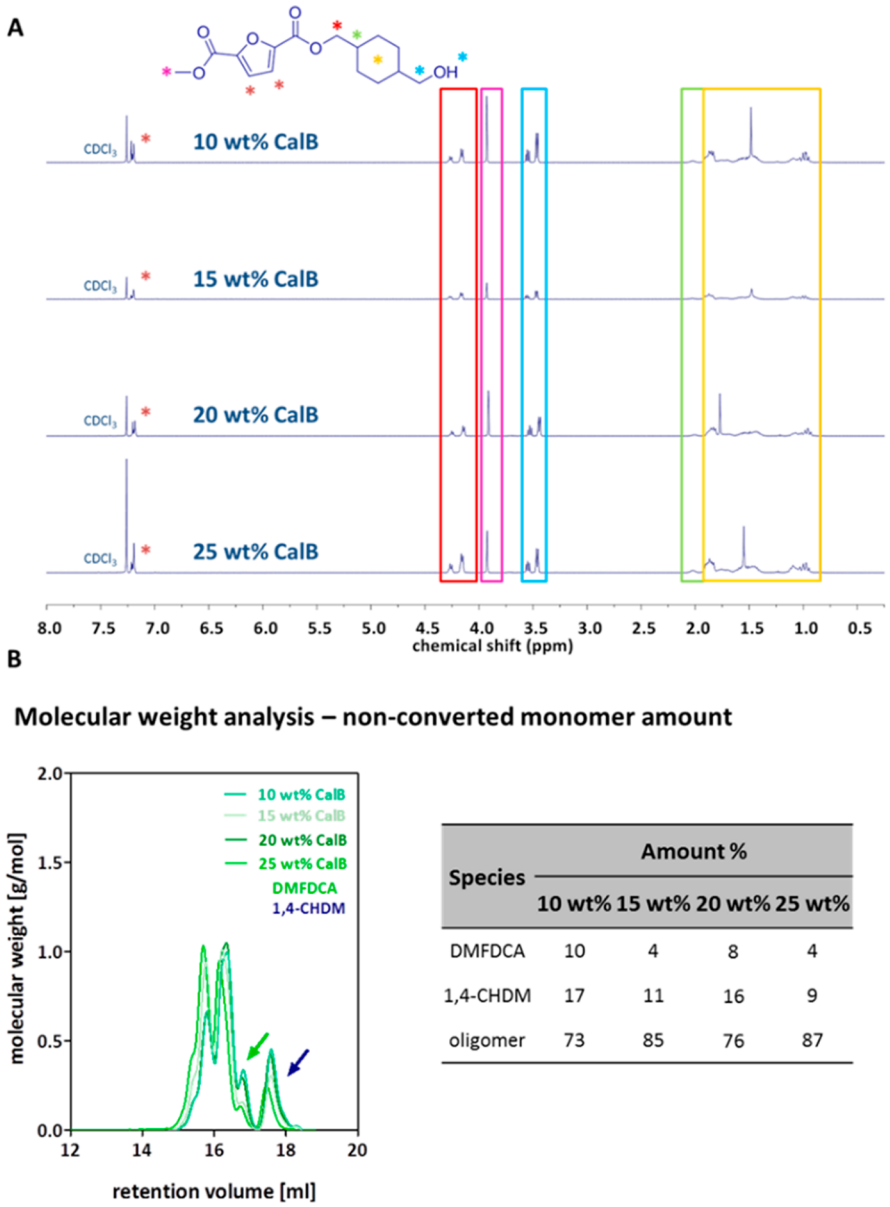

Species	Amount %			
	10 wt%	15 wt%	20 wt%	25 wt%
DMFDCA	10	4	8	4
1,4-CHDM	17	11	16	9
oligomer	73	85	76	87

Figure 10. Results of polycondensation of dimethyl furan-2,5-dicarboxylate with 1,4-cyclohexanedimethanol. (A) Comparison of ^{1}H-NMR spectra of poly(methoxycyclohexyl) furanoates generated with reduced enzyme amounts. Peaks are indicated with boxes colored to the corresponding asterisk for structural assignment. (B) Monomer and oligofuranoate calculation within the poly(methoxycyclohexyl) furanoates. The GPC elugram is shown, and peaks of nonconverted DMFDCA and 1,4-CHDM are indicated. Calculated nonconverted monomer and oligofuranoate amounts are shown.

polycondensation with 15 and 25 wt % of enzyme for additional two times. Here, yields are varying between 93% to 96% when 15 wt % enzyme is applied and between 60% and 92% when 25 wt % are used. The more consistent oligofuranoate yields above 90% using 15 wt % CalB can be explained by the previously mentioned issue of viscosity or miscibility if diffusion control of the reaction is assumed. A lower amount of enzyme beads gives a lower overall viscosity and is more easily mixed with the monomers for successful polycondensation. In conclusion, the synthesis of 1,4-CHDM oligofuranoate is improved with a reduced amount of 15 wt % immobilized CalB.

After the successful reduction of the enzyme used (15 wt %) for high 1,4-CHDM oligofuranoate product yield (>90%), it was tested if costs can be further decreased by recycling of the enzyme. Immobilized CalB was used in two different ways: First, the enzyme was used more or less directly for an additional polycondensation. Second, it was washed with 1-butanol before reuse.

1-Butanol is a hydrophilic, polar solvent (log P = 0.79). It was chosen because a previous study of immobilized CalB reuse for biodiesel synthesis showed the highest product yield for enzyme recycling when it was washed with it.[85] Immobilized CalB was recycled twice in the 1,4-CHDM oligofuranoate synthesis. The previously established experimental protocol using 15 wt % of enzyme was applied. As all previous experiments showed similar oligofuranoate characteristics concerning the generated end groups and the thermal behavior, the 1,4-CHDM oligomers produced with recycled immobilized CalB were only analyzed by ^{1}H NMR spectroscopy to verify oligofuranoate synthesis and by gel permeation chromatography to calculate the non-converted monomer amount and subsequently the oligofuranoate product yield. Results from ^{1}H NMR measurements

DOI: 10.1021/acssuschemeng.9b05874
ACS Sustainable Chem. Eng. 2020, 8, 1068−1086

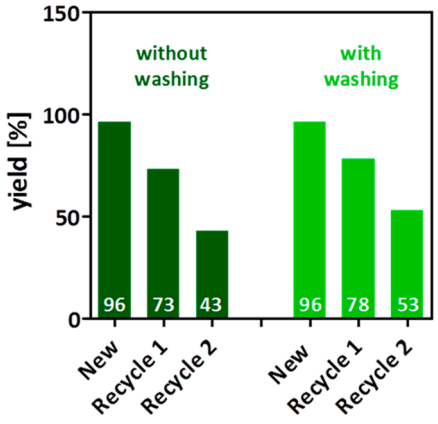

Figure 11. 1,4-CHDM oligofuranoate product yield after recycling of immobilized CalB. Oligofuranoate yields are shown according to the two applied methods for immobilized CalB recycling (without washing and with washing) and the subsequent three consecutive polycondensations of dimethyl furan-2,5-dicarboxylate with 1,4-cyclohexanedimethanol. 1,4-CHDM oligofuranoates synthesized with new immobilized CalB (New), with one time previously used immobilized CalB (Recycle 1), and with two times previously used immobilized CalB (Recycle 2).

indicate that 1,4-CHDM oligofuranoates were produced in all batches for both of the applied methods for CalB recycling. The oligofuranoate yield decreases around 20% with each additional reuse of immobilized CalB (Figure 11). This is in contrast to the previously mentioned study of immobilized CalB reuse for biodiesel synthesis. This showed a drop in product yield of about 60% in the second reuse of nonwashed immobilized CalB and a further 20% decrease within the third reuse.[85] Here, no significant difference in oligofuranoate product yield has been observed when reusing either the nonwashed or the washed immobilized CalB. The difference between a DMFDCA/CHDM reaction and biodiesel production is that that during the latter glycerol is produced as a byproduct. This blocks the active site of immobilized CalB and hampers its catalytic activity when not removed by washing with a hydrophilic, polar solvent as for example 1-butanol.[85] During the polycondensation of DMFDCA and 1,4-CHDM, no such byproduct is produced. Therefore, no difference in product yield is observed when immobilized CalB is not washed with 1-butanol prior to reuse. These results show that the recycling of immobilized CalB without further treatment indeed is possible but results in a decrease in oligofuranoate yield of about 20% with each additional reuse.

For optimizing the synthesis of 1,4-CHDM oligofuranoates, all experimental parameters were targeted. This started with changing the reaction system to a solvent-free one, reducing the polycondensation time, and varying the polycondensation temperature to finally reduce the most cost-intensive enzyme amount applied for oligofuranoate synthesis. Figure 12 summarizes the best experimental set up and the achieved results. The use of 15 wt % immobilized CalB, a monomer ratio of 2:3 in a solvent-free system for polycondensation at 80 °C for initially 2 h under nitrogen atmosphere, and additionally 24 h under high vacuum (2 mmHg) (Figure 12B) resulted in 95% yield of an easy to handle and analyze 1,4-CHDM oligofuranoate with a majority of Ester/OH and OH/OH end groups (Figure 12C, molecular weight analysis, microstructure analysis). This highly pure oligofuranoate (monomer amount 11%, Figure 12C, monomer/oligomer amount) shows a decomposition start around 180 °C reaching its maximum around 265 and 390 °C (Figure 12C, molecular weight analysis, microstructure analysis). The melting temperature range is between 111 and 213 °C and crystallization at 116 °C.

Finally, it was studied if the developed synthetic procedure is applicable for the large-scale production of 1,4-CHDM oligofuranoate oligomer diols. Although final optimization approaches regarding the necessary enzyme amount for high yields of 1,4-CHDM oligofuranoate showed that 15 wt % of immobilized CalB is the most suitable one, for the large-scale production of 1,4-CHDM oligofuranoate 25 wt % were applied because these two approaches were performed in parallel.

The large-scale polycondensation was performed according to the best experimental set up but with 25 wt % immobilized CalB instead of 15 wt %, and the amounts of all reaction components were increased 20-fold. As all previously synthesized oligomers, the oligofuranoate produced in large scale was verified, analyzed, and characterized by the previously mentioned methods. The successful production of the 1,4-CHDM oligofuranoate is not only possible in small scale but also in large scale (Figure 13A, red boxes), as indicated by the chemical shift of the proton peaks from the formed ester bond during polycondensation. Also, regarding the molecular weight, the microstructure and thermal behavior of the oligofuranoate synthesized in large scale showed similar properties to the one generated in small scale. The only differences in the oligofuranotes of these two approaches are observed in the nonconverted monomer and the oligomer amount. Here, the large-scale system resulted in only 63% of the oligomer with a total remaining monomer amount of 37% (Figure 13B, table). Compared to the small-scale system, this means a calculated oligomer loss of 24% (Figure 13B, table) with a total yield loss of 11%.

This comes along with a significantly higher nonconverted amount of 1,4-CHDM (35%) in the large-scale system compared to only 9% in the small scale system (Figure 13B, table).

This observation can be explained by the already mentioned reduced miscibility of all reaction components in this solvent-free system. This already hampered miscibility is even higher in the large-scale system based on the 20-fold increase in the amount of all components. Nevertheless, with this large-scale production, it was possible to synthesize a total amount of 42 g of oligofuranoate/nonconverted monomer suspension including 26 g of 1,4-CHDM oligofuranoate.

CONCLUSION

The enzymatic synthesis of oligomer diols comprising furans with high end-group fidelity is a promising approach for introducing highly temperature-sensitive furans in polycondensates and might provide improved flame-retardant properties to the resulting polymers. The use of an enzymatic catalyst, especially the use of the immobilized lipase B from *Candida antarctica* (CalB) (Novozym 435), for the synthesis of different furan polymers and oligomers has been intensively studied and successfully performed.[69−74] In contrast to these studies that were focused on exploring a wide range of diols and diamines regarding high molecular weight furan polymers, the current work aimed at the generation of furan oligomers which syntheses and yields fulfill the industrial requirements for subsequent polycondensation.

Using a DMFDCA 1,4-CHDM ratio of 2:3 with 15 wt % of CalB in a solvent-free system for two-stage polycondensation, that includes 2 h of oligomerization under a nitrogen

DOI: 10.1021/acssuschemeng.9b05874
ACS Sustainable Chem. Eng. 2020, 8, 1068−1086

A

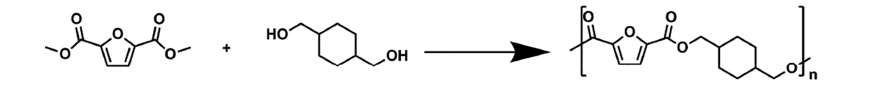

dimethyl furan-2,5-dicarboxylate 1,4-cyclohexanedimethanol (cis/trans mixture) poly(methoxycyclohexyl) furanoate (PMCF)

B

parameters	Best experimental set up
Monomer amount	30 % of total reaction volume
Monomer ratio	2:3
Enzyme amount/Lewatit beads amount	15 wt%
Solvent	-
Solvent amount	0 wt %
Temperature	80 °C
Time	2/24 h
Surrounding (N_2,vacuum)	N_2/2 mmHg

C

Molecular weight analysis

Yield %	GPC $\overline{M_n}$	GPC $\overline{M_w}$	Đ
95 ± 1,7	620 ± 71	817 ± 104	1.3

Monomer/Oligomer amount

Species	Amount %
DMFDCA	4
1,4-CHDM	7 ± 3,6
oligomer	89 ± 3,8

Microstructure analysis

End groups		
1st	2nd	3rd
Ester/OH	OH/OH	Ester/OH

Thermal analysis

$T_{d\text{-}5\%}$ [°C]	$T_{d\text{-}max}$ [°C]	T_g [°C]	T_m [°C]	T_c [°C]	T_{cc} [°C]
183 ± 13	265/390 ± 10/6	-	111-213 ± 5-14	116 ± 5	-

Figure 12. Best experimental set up for 1,4-CHDM oligofuranoate synthesis. (A) Polycondensation of dimethyl furan-2,5-dicarboxylate with 1,4-cyclohexanedimethanol. Polycondensation of dimethyl furan-2,5-dicarboxylate with 1,4-cyclohexanedimethanol (cis/trans mixture) to generate poly(methoxycyclohexyl)furanoate was performed via a two-stage method using immobilized CalB as the enzymatic catalyst. (B) Experimental set up of polycondensation. DMFDCA and 1,4-CHDM react in a 2:3 monomer ratio, with 10 wt % of immobilized CalB and without a reaction solvent in a two-stage polycondensation reaction at 80 °C for 24 h. The first stage is performed at 80 °C for 2 h under a nitrogen atmosphere and the second one at reduced pressure of 2 mmHg for an additional 24 h. The wt % of immobilized CalB and the reaction solvent were calculated based on the total monomer in g. (C) Characterization of 1,4-CHDM oligofuranoate synthesized with the best experimental set up. Molecular weight analysis: Experimental number, used monomer ratio, calculated yield, number-average ($\overline{M_n}$) calculated via ^{1}H NMR and GPC, weight-average ($\overline{M_w}$) molecular weight (g/mol) determined via GPC, and calculated dispersity are shown. Microstructure analysis: End groups identified via ESI-HRMS are classified according to the HRMS peak intensity of the corresponding measured molecular weight for this end group species. Thermal analysis: Experimental number, used monomer ratio, temperature of 5% weight loss ($T_{d\text{-}5\%}$), highest weight loss rate% per temperature °C, indicating the maximum rate of decomposition ($T_{d\text{-}max}$), glass transition temperature (T_g), melting temperature (T_m), crystallization (T_c), and cold crystallization (T_{cc}) are shown.

atmosphere and an additional 24 h under high vacuum at 80 °C, an oligofuranoate diol with excellent end-group fidelity and a yield of 95% was successfully synthesized. Recycling of immobilized CalB to further decrease the cost effort of using an enzymatic catalyst is possible but showed limitations in the product yield that further decreases about 20% with each additional reuse.

Investigations on the polycondensation of the generated 1,4-CHDM oligofuranoate diols with commercial diacids and diisocyanates via solution and melt polycondensation are currently conducted to build a new material platform using the developed diols.

AUTHOR INFORMATION

Corresponding Author

*E-mail: k.u.loos@rug.nl. Phone: +31-50 363 6867.

ORCID

Katja Loos: 0000-0002-4613-1159

Present Address

§P. Skoczinski: nova-Institut GmbH, Chemiepark Knapsack, Industriestraße 300, 50354 Hürth, Germany

Author Contributions

The manuscript was written through contributions of all authors. All authors have given approval to the final version of the manuscript.

DOI: 10.1021/acssuschemeng.9b05874
ACS Sustainable Chem. Eng. 2020, 8, 1068−1086

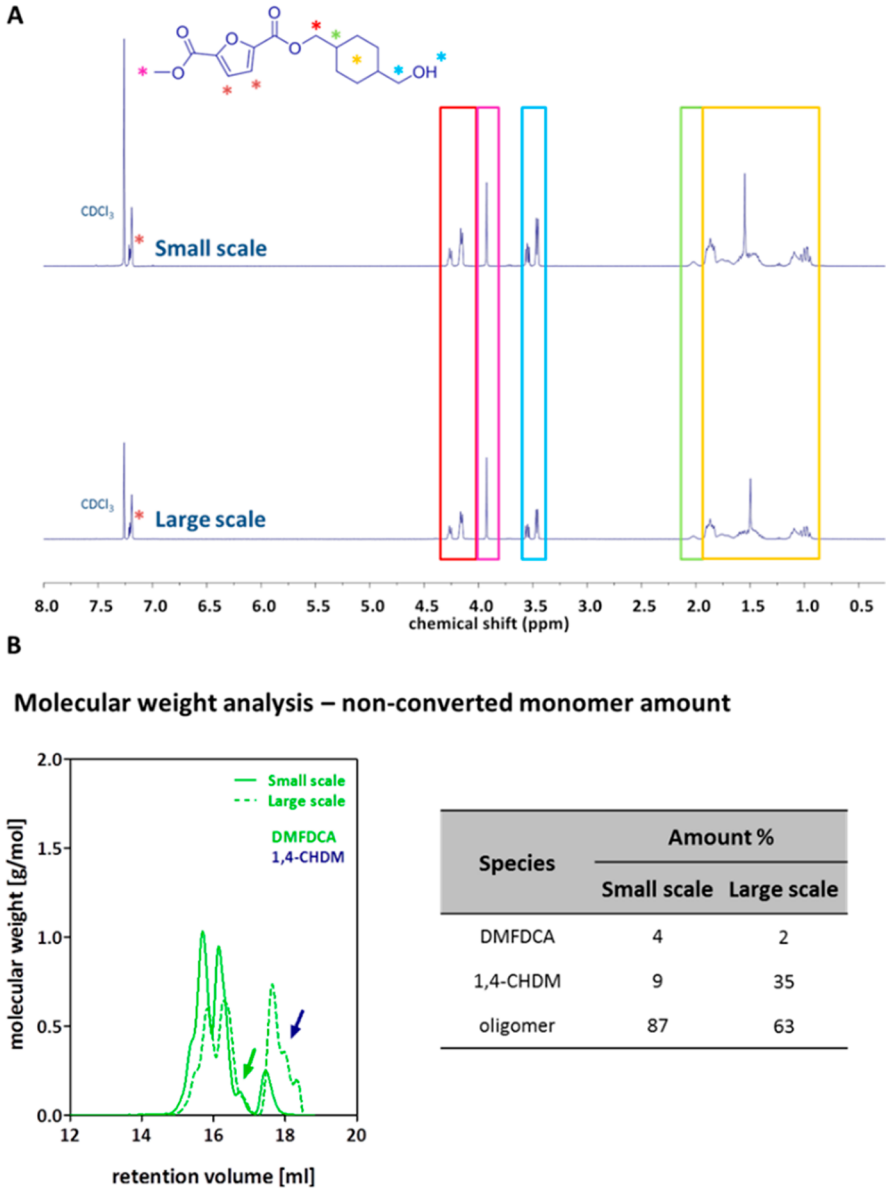

Species	Amount %	
	Small scale	Large scale
DMFDCA	4	2
1,4-CHDM	9	35
oligomer	87	63

Figure 13. Results of large-scale polycondensation of dimethyl furan-2,5-dicarboxylate with 1,4-cyclohexanedimethanol. (A) Comparison of ^{1}H NMR spectra of poly(methoxycyclohexyl) furanoates generated in small and large scale. Peaks are indicated with boxes colored to the corresponding asterisk for structural assignment. (B) Monomer and oligofuranoate calculation within the poly(methoxycyclohexyl) furanoates. The GPC elugram is shown, and peaks of nonconverted DMFDCA and 1,4-CHDM are indicated. Calculated nonconverted monomer and oligofuranoate amounts are shown.

Notes

The authors declare no competing financial interest.

■ ACKNOWLEDGMENTS

We would like to acknowledge Albert Woortman for GPC measurements, Jur van Dijken for performing the thermal gravimetric analysis (TGA) measurements, and Annie van Dam and Marcel de Vries of the Mass Spectrometry Core Facility of the Faculty of Science and Engineering (Analytical Biochemistry, Groningen Research Institute of Pharmacy, Antonius Deusinglaan 1, 9713 AV Groningen) for executing and evaluating the ESI-HRMS measurements. This research was financially supported by Covestro AG, Germany. Dina Maniar gratefully acknowledges the financial support from the Indonesian Endowment Fund for Education (Lembaga Pengelola Dana Pendidikan LPDP).

■ REFERENCES

(1) Marrucci, L.; Daddi, T.; Iraldo, F. The integration of circular economy with sustainable consumption and production tools: Systematic review and future research agenda. *J. Cleaner Prod.* **2019**, *240*, 118268.

(2) Keijer, T.; Bakker, V.; Slootweg, J. C. Circular chemistry to enable a circular economy. *Nat. Chem.* **2019**, *11*, 190−195.

(3) Nakajima, H.; Dijkstra, P.; Loos, K. The Recent Developments in Biobased Polymers toward General and Engineering Applications: Polymers that Are Upgraded from Biodegradable Polymers, Analogous to Petroleum-Derived Polymers, and Newly Developed. *Polymers* **2017**, *9*, 523.

(4) Gandini, A.; Belgacem, M. N. Furans in polymer chemistry. *Prog. Polym. Sci.* **1997**, *22*, 1203−1379.

(5) Gandini, A. Monomers and Macromonomers from Renewable Resources. In *Biocatalysis in Polymer Chemistry*; Loos, K., Ed.; Wiley-VCH Verlag GmbH & Co. KGaA, 2010; pp 1−33.

DOI: 10.1021/acssuschemeng.9b05874
ACS Sustainable Chem. Eng. 2020, 8, 1068−1086

(6) Gandini, A. Furans as offspring of sugars and polysaccharides and progenitors of a family of remarkable polymers: A review of recent progress. *Polym. Chem.* **2010**, *1*, 245−251.
(7) Corma, A.; Iborra, S.; Velty, A. Chemical Routes for the Transformation of Biomass into Chemicals. *Chem. Rev.* **2007**, *107*, 2411−2502.
(8) Román-Leshkov, Y.; Chheda, J. N.; Dumesic, J. A. Phase Modifiers Promote Efficient Production of Hydroxymethylfurfural from Fructose. *Science* **2006**, *312*, 1933−1937.
(9) Bicker, M.; Hirth, J.; Vogel, H. Dehydration of fructose to 5-hydroxymethylfurfural in sub- and supercritical acetone. *Green Chem.* **2003**, *5*, 280−284.
(10) Moreau, C.; Belgacem, M. N.; Gandini, A. Recent catalytic advances in the chemistry of substituted furans from carbohydrates and in the ensuing polymers. *Top. Catal.* **2004**, *27*, 11−30.
(11) Isikgor, F. H.; Becer, C. R. Lignocellulosic biomass: a sustainable platform for the production of bio-based chemicals and polymers. *Polym. Chem.* **2015**, *6*, 4497−4559.
(12) Vilela, C.; Sousa, A. F.; Fonseca, A. C.; Serra, A. C.; Coelho, J. F. J.; Freire, C. S. R.; Silvestre, A. J. D. The quest for sustainable polyesters - insights into the future. *Polym. Chem.* **2014**, *5*, 3119−3141.
(13) Araujo, C. F.; Nolasco, M. M.; Ribeiro-Claro, P. J. A.; Rudic, S.; Silvestre, A. J. D.; Vaz, P. D.; Sousa, A. F. Inside PEF: Chain Conformation and Dynamics in Crystalline and Amorphous Domains. *Macromolecules* **2018**, *51*, 3515−3526.
(14) Hu, H.; Zhang, R. Y.; Sousa, A.; Long, Y.; Ying, W. B.; Wang, J. G.; Zhu, J. Bio-based poly(butylene 2,5-furandicarboxylate)-b-poly-(ethylene glycol) copolymers with adjustable degradation rate and mechanical properties: Synthesis and echaracterization. *Eur. Polym. J.* **2018**, *106*, 42−52.
(15) Matos, M.; Cordeiro, R. A.; Faneca, H.; Coelho, J. F. J.; Silvestre, A. J. D.; Sousa, A. F. Replacing Di(2-ethylhexyl) Terephthalate by Di(2-ethylhexyl) 2,5-Furandicarboxylate for PVC Plasticization: Synthesis, Materials Preparation and Characterization. *Materials* **2019**, *12*, 2336.
(16) Matos, M.; Sousa, A. F.; Mendonca, P. V.; Silvestre, A. J. D. Co-Polymers based on Poly(1,4-butylene 2,5-furandicarboxylate) and Poly(propylene oxide) with Tuneable Thermal Properties: Synthesis and Characterization. *Materials* **2019**, *12*, 328.
(17) Sousa, A. F.; Guigo, N.; Pozycka, M.; Delgado, M.; Soares, J.; Mendonca, P. V.; Coelho, J. F. J.; Sbirrazzuoli, N.; Silvestre, A. J. D. Tailored design of renewable copolymers based on poly(1,4-butylene 2,5-furandicarboxylate) and poly(ethylene glycol) with refined thermal properties. *Polym. Chem.* **2018**, *9*, 722−731.
(18) Zaidi, S.; Thiyagarajan, S.; Bougarech, A.; Sebti, F.; Abid, S.; Majdi, A.; Silvestre, A. J. D.; Sousa, A. F. Highly transparent films of new copolyesters derived from terephthalic and 2,4-furandicarboxylic acids. *Polym. Chem.* **2019**, *10*, 5324−5332.
(19) Genovese, L.; Soccio, M.; Lotti, N.; Munari, A.; Szymczyk, A.; Paszkiewicz, S.; Linares, A.; Nogales, A.; Ezquerra, T. A. Effect of chemical structure on the subglass relaxation dynamics of biobased polyesters as revealed by dielectric spectroscopy: 2,5-furandicarboxylic acid vs. trans-1,4-cyclohexanedicarboxylic acid. *Phys. Chem. Chem. Phys.* **2018**, *20*, 15696−15706.
(20) Gigli, M.; Quartinello, F.; Soccio, M.; Pellis, A.; Lotti, N.; Guebitz, G. M.; Licoccia, S.; Munari, A. Enzymatic hydrolysis of poly(1,4-butylene 2,5-thiophenedicarboxylate) (PBTF) and poly(1,4-butylene 2,5-furandicarboxylate) (PBF) films: A comparison of mechanisms. *Environ. Int.* **2019**, *130*, 104852.
(21) Guidotti, G.; Genovese, L.; Soccio, M.; Gigli, M.; Munari, A.; Siracusa, V.; Lotti, N. Block Copolyesters Containing 2,5-Furan and trans-1,4-Cyclohexane Subunits with Outstanding Gas Barrier Properties. *Int. J. Mol. Sci.* **2019**, *20*, 2187.
(22) Maini, L.; Gigli, M.; Gazzano, M.; Lotti, N.; Bikiaris, D. N.; Papageorgiou, G. Z. Structural Investigation of Poly(ethylene furanoate) Polymorphs. *Polymers* **2018**, *10*, 296.
(23) Gandini, A.; Lacerda, T. M.; Carvalho, A. J.; Trovatti, E. Progress of Polymers from Renewable Resources: Furans, Vegetable Oils, and Polysaccharides. *Chem. Rev.* **2016**, *116*, 1637−1669.
(24) Kandola, B.; Krishnan, L. Fire Performance Evaluation of Different Resins for Potential Application in Fire Resistant Structural Marine Composites. *Fire Safety Science* **2014**, *11*, 769−780.
(25) Cohen, K.; Menon, S. Method for producing polyester polyols. ; European Patent EP 3212691 B1, 30.10.2015.
(26) Meng, J. J.; Zeng, Y. S.; Zhu, G. Q.; Zhang, J.; Chen, P. F.; Cheng, Y.; Fang, Z.; Guo, K. Sustainable bio-based furan epoxy resin with flame retardancy. *Polym. Chem.* **2019**, *10*, 2370−2375.
(27) Bilal, M.; Adeel, M.; Rasheed, T.; Zhao, Y. P.; Iqbal, H. M. N. Emerging contaminants of high concern and their enzyme-assisted biodegradation - A review. *Environ. Int.* **2019**, *124*, 336−353.
(28) Liagkouridis, L.; Cousins, A. P.; Cousins, I. T. Physical-chemical properties and evaluative fate modelling of 'emerging' and 'novel' brominated and organophosphorus flame retardants in the indoor and outdoor environment. *Sci. Total Environ.* **2015**, *524*, 416−426.
(29) Richardson, S. D.; Kimura, S. Y. Emerging environmental contaminants: Challenges facing our next generation and potential engineering solutions. *Environmental Technology & Innovation* **2017**, *8*, 40−56.
(30) Wei, G. L.; Li, D. Q.; Zhuo, M. N.; Liao, Y. S.; Xie, Z. Y.; Guo, T. L.; Li, J. J.; Zhang, S. Y.; Liang, Z. Q. Organophosphorus flame retardants and plasticizers: Sources, occurrence, toxicity and human exposure. *Environ. Pollut.* **2015**, *196*, 29−46.
(31) Li, S.; Yan, H. X.; Feng, S. Y.; Li, X. Phosphorus-containing flame-retardant bismaleimide resin with high mechanical properties. *Polym. Bull.* **2016**, *73*, 3547−3557.
(32) Morgan, A. B. The Future of Flame Retardant Polymers - Unmet Needs and Likely New Approaches. *Polym. Rev.* **2019**, *59*, 25−54.
(33) Wendels, S.; Chavez, T.; Bonnet, M.; Salmeia, K. A.; Gaan, S. Recent Developments in Organophosphorus Flame Retardants Containing P-C Bond and Their Applications. *Materials* **2017**, *10*, 784.
(34) Konieczny, J.; Loos, K. Bio-based polyurethane films using white dextrins. *J. Appl. Polym. Sci.* **2019**, *136*, 47454.
(35) Konieczny, J.; Loos, K. Polyurethane Coatings Based on Renewable White Dextrins and Isocyanate Trimers. *Macromol. Rapid Commun.* **2019**, *40*, 1800874.
(36) Konieczny, J.; Loos, K. Green Polyurethanes from Renewable Isocyanates and Biobased White Dextrins. *Polymers* **2019**, *11*, 256.
(37) Halacheva, N.; Novakov, P. Preparation of oligoester diols by alcoholytic destruction of poly(ethylene terephthalate). *Polymer* **1995**, *36*, 867−874.
(38) Çam, C.; Bal, A.; Güçlü, G. Synthesis and film properties of epoxy esters modified with amino resins from glycolysis products of postconsumer PET bottles. *Polym. Eng. Sci.* **2015**, *55*, 2519−2525.
(39) Hoang, C. N.; Pham, C. T.; Dang, T. M.; Hoang, D. Q.; Lee, P. C.; Kang, S. J.; Kim, J. Novel oligo-ester-ether-diol prepared by waste poly(ethylene terephthalate) glycolysis and its use in preparing thermally stable and flame retardant polyurethane foam. *Polymers* **2019**, *11*, 236.
(40) Luo, X.; Li, Y. Synthesis and Characterization of Polyols and Polyurethane Foams from PET Waste and Crude Glycerol. *J. Polym. Environ.* **2014**, *22*, 318−328.
(41) Mazurek, M. M.; Tomczyk, K.; Rokicki, G. PET wastes utilization in the synthesis of aliphatic-aromatic polyurethane elastomers. *Polym. Adv. Technol.* **2014**, *25*, 1273−1284.
(42) Báez, J. E.; Marcos-Fernández, Á.; Navarro, R. Similarities between homopolymers and triblock copolymers derived from poly(ε-caprolactone) (PCL) macrodiols (HOPCL-E-PCLOH and HOPCL-PEG-PCLOH) and their poly(ester-ether-urethanes): synthesis and characterization. *Chemical Papers* **2019**, *73*, 1287−1299.
(43) Adrio, J. L.; Demain, A. L. Microbial enzymes: tools for biotechnological processes. *Biomolecules* **2014**, *4*, 117−39.
(44) Loos, K., Ed.; *Biocatalysis in Polymer Chemistry*; Wiley, 2010.
(45) Gross, R. A.; Kumar, A.; Kalra, B. Polymer Synthesis by In Vitro Enzyme Catalysis. *Chem. Rev.* **2001**, *101*, 2097−2124.
(46) Kobayashi, S., Uyama, H., Kadokawa, J.-i., Eds.; *Enzymatic Polymerization towards Green Polymer Chemistry*; Springer: Singapore, 2019.

DOI: 10.1021/acssuschemeng.9b05874
ACS Sustainable Chem. Eng. 2020, 8, 1068−1086

(47) Kobayashi, S.; Uyama, H.; Kimura, S. Enzymatic Polymerization. *Chem. Rev.* **2001**, *101*, 3793−3818.
(48) Bruns, N., Loos, K., Eds.; *Enzymatic Polymerizations*; Elsevier, 2019; Vol. 627.
(49) Gong, J. S.; Lu, Z. M.; Li, H.; Shi, J. S.; Zhou, Z. M.; Xu, Z. H. Nitrilases in nitrile biocatalysis: recent progress and forthcoming research. *Microb. Cell Fact.* **2012**, *11*, 142.
(50) Loos, K.; Jonas, G.; Stadler, R. Carbohydrate modified polysiloxanes, 3 - Solution properties of carbohydrate-polysiloxane conjugates in toluene. *Macromol. Chem. Phys.* **2001**, *202*, 3210−3218.
(51) Loos, K.; Stadler, R. Synthesis of amylose-block-polystyrene rod-coil block copolymers. *Macromolecules* **1997**, *30*, 7641−7643.
(52) Loos, K.; von Braunmühl, V.; Stadler, R.; Landfester, K.; Spiess, H. W. Saccharide modified silica particles by enzymatic grafting. *Macromol. Rapid Commun.* **1997**, *18*, 927−938.
(53) Adharis, A.; Ketelaar, T.; Komarudin, A. G.; Loos, K. Synthesis and Self-Assembly of Double-Hydrophilic and Amphiphilic Block Glycopolymers. *Biomacromolecules* **2019**, *20*, 1325−1333.
(54) Adharis, A.; Loos, K. Green Synthesis of Glycopolymers Using an Enzymatic Approach. *Macromol. Chem. Phys.* **2019**, *220*, 1900219.
(55) Adharis, A.; Petrovic, D. M.; Ozdamar, I.; Woortman, A. J. J.; Loos, K. Environmentally friendly pathways towards the synthesis of vinyl-based oligocelluloses. *Carbohydr. Polym.* **2018**, *193*, 196−204.
(56) Adharis, A.; Vesper, D.; Koning, N.; Loos, K. Synthesis of (meth)acrylamide-based glycomonomers using renewable resources and their polymerization in aqueous systems. *Green Chem.* **2018**, *20*, 476−484.
(57) Kloosterman, W. M. J.; Brouwer, S. G. M.; Loos, K. Enzyme-Catalyzed Synthesis of Saccharide Acrylate Monomers from Nonedible Biomass. *Chem. - Asian J.* **2014**, *9*, 2156−2161.
(58) Kloosterman, W. M. J.; Jovanovic, D.; Brouwer, S. G. M.; Loos, K. Amylase catalyzed synthesis of glycosyl acrylates and their polymerization. *Green Chem.* **2014**, *16*, 203−210.
(59) Kloosterman, W. M. J.; Roest, S.; Priatna, S. R.; Stavila, E.; Loos, K. Chemo-enzymatic synthesis route to poly(glucosyl-acrylates) using glucosidase from almonds. *Green Chem.* **2014**, *16*, 1837−1846.
(60) Kloosterman, W. M. J.; Spoelstra-van Dijk, G.; Loos, K. Biocatalytic Synthesis of Maltodextrin-Based Acrylates from Starch and alpha-Cyclodextrin. *Macromol. Biosci.* **2014**, *14*, 1268−1279.
(61) Maurer, K. H.; Elleuche, S.; Antranikian, G. Enzyme. In *Industrielle Mikrobiologie*; Sahm, H.; Antranikian, G.; Stahmann, K.-P.; Takors, R., Eds.; Springer Spektrum, 2013.
(62) Jiang, Y.; Woortman, A. J. J.; van Ekenstein, G. O. R. A.; Loos, K. A biocatalytic approach towards sustainable furanic-aliphatic polyesters. *Polym. Chem.* **2015**, *6*, 5198−5211.
(63) Jaeger, K. E.; Reetz, M. T. Microbial lipases form versatile tools for biotechnology. *Trends Biotechnol.* **1998**, *16*, 396−403.
(64) Ali, Y. B.; Verger, R.; Abousalham, A. Lipases or Esterases: Does It Really Matter? Toward a New Bio-Physico-Chemical Classification. In *Lipases and Phospholipases: Methods and Protocols*; Sandoval, G., Ed.; Humana Press: Totowa, NJ, 2012; pp 31−51.
(65) Anderson, E. M.; Larsson, K. M.; Kirk, O. One Biocatalyst-Many Applications: The Use of *Candida antarctica* B-Lipase in Organic Synthesis. *Biocatal. Biotransform.* **1998**, *16*, 181−204.
(66) Warwel, S.; Steinke, G.; Klaas, M. R. g. An efficient method for lipase-catalysed preparation of acrylic and methacrylic acid esters. *Biotechnol. Tech.* **1996**, *10*, 283−286.
(67) de Goede, A. T. J. W.; van Oosterom, M.; van Deurzen, M. P. J.; Sheldon, R. A.; van Bekkum, H.; van Rantwijk, F. Selective Acylation of Sugar Derivatives Catalyzed by Immobilized Lipase. *Stud. Surf. Sci. Catal.* **1993**, *78*, 513−520.
(68) Geyer, U.; Klemm, D.; Pavel, K.; Ritter, H. Enzymes in polymer chemistry, 8 Chemoenzymatic synthesis of polymerizable 11-methacryloyl-aminoundecanoic ester of 1- and 3-O-methyl-α-D-glucose in 6-O-position. *Macromol. Rapid Commun.* **1995**, *16*, 337−341.
(69) Jiang, Y.; Woortman, A. J.; van Ekenstein, G. O.; Loos, K. Enzyme-catalyzed synthesis of unsaturated aliphatic polyesters based on green monomers from renewable resources. *Biomolecules* **2013**, *3*, 461−80.
(70) Jiang, Y.; Woortman, A. J.; Alberda van Ekenstein, G. O.; Petrovic, D. M.; Loos, K. Enzymatic synthesis of biobased polyesters using 2,5-bis(hydroxymethyl)furan as the building block. *Biomacromolecules* **2014**, *15*, 2482−93.
(71) Jiang, Y.; Loos, K. Enzymatic Synthesis of Biobased Polyesters and Polyamides. *Polymers* **2016**, *8*, 243.
(72) Jiang, Y.; Maniar, D.; Woortman, A. J. J.; Loos, K. Enzymatic synthesis of 2,5-furandicarboxylic acid-based semi-aromatic polyamides: enzymatic polymerization kinetics, effect of diamine chain length and thermal properties. *RSC Adv.* **2016**, *6*, 67941−67953.
(73) Jiang, Y.; Maniar, D.; Woortman, A. J.; Alberda van Ekenstein, G. O.; Loos, K. Enzymatic Polymerization of Furan-2,5-Dicarboxylic Acid-Based Furanic-Aliphatic Polyamides as Sustainable Alternatives to Polyphthalamides. *Biomacromolecules* **2015**, *16*, 3674−85.
(74) Jiang, Y.; Maniar, D.; Woortman, A. J. J.; Alberda van Ekenstein, G. O. R.; Loos, K. Enzymatic Polymerization of Furan-2,5-Dicarboxylic Acid-Based Furanic-Aliphatic Polyamides as Sustainable Alternatives to Polyphthalamides. *Biomacromolecules* **2015**, *16*, 3674−3685.
(75) Maniar, D.; Hohmann, K. F.; Jiang, Y.; Woortman, A. J. J.; van Dijken, J.; Loos, K. Enzymatic Polymerization of Dimethyl 2,5-Furandicarboxylate and Heteroatom Diamines. *Acs Omega* **2018**, *3*, 7077−7085.
(76) Maniar, D.; Jiang, Y.; Woortman, A. J. J.; van Dijken, J.; Loos, K. Furan-Based Copolyesters from Renewable Resources: Enzymatic Synthesis and Properties. *ChemSusChem* **2019**, *12*, 990−999.
(77) Schwab, L. W.; Kroon, R.; Schouten, A. J.; Loos, K. Enzyme-Catalyzed Ring-Opening Polymerization of Unsubstituted β-Lactam. *Macromol. Rapid Commun.* **2008**, *29*, 794−797.
(78) Stavila, E.; Arsyi, R. Z.; Petrovic, D. M.; Loos, K. Fusarium solani pisi cutinase-catalyzed synthesis of polyamides. *Eur. Polym. J.* **2013**, *49*, 834−842.
(79) Stavila, E.; Loos, K. Synthesis of lactams using enzyme-catalyzed aminolysis. *Tetrahedron Lett.* **2013**, *54*, 370−372.
(80) Stavila, E.; van Ekenstein, G.; Woortman, A. J. J.; Loos, K. Lipase-Catalyzed Ring-Opening Copolymerization of epsilon-Caprolactone and beta-Lactam. *Biomacromolecules* **2014**, *15*, 234−241.
(81) Stavila, E.; van Ekenstein, G. O. R. A.; Loos, K. Enzyme-Catalyzed Synthesis of Aliphatic-Aromatic Oligoamides. *Biomacromolecules* **2013**, *14*, 1600−1606.
(82) Izunobi, J. U.; Higginbotham, C. L. Polymer Molecular Weight Analysis by ^{1}H NMR Spectroscopy. *J. Chem. Educ.* **2011**, *88*, 1098−1104.
(83) Kasmi, N.; Majdoub, M.; Papageorgiou, G. Z.; Bikiaris, D. N. Synthesis and crystallization of new fully renewable resources-based copolyesters: Poly(1,4-cyclohexanedimethanol-co-isosorbide 2,5-furandicarboxylate). *Polym. Degrad. Stab.* **2018**, *152*, 177−190.
(84) Tsanaktsis, V.; Vouvoudi, E.; Papageorgiou, G. Z.; Papageorgiou, D. G.; Chrissafis, K.; Bikiaris, D. N. Thermal degradation kinetics and decomposition mechanism of polyesters based on 2,5-furandicarboxylic acid and low molecular weight aliphatic diols. *J. Anal. Appl. Pyrolysis* **2015**, *112*, 369−378.
(85) Aguieiras, E. C.; Ribeiro, D. S.; Couteiro, P. P.; Bastos, C. M.; de Queiroz, D. S.; Parreira, J. M.; Langone, M. A. Investigation of the Reuse of Immobilized Lipases in Biodiesel Synthesis: Influence of Different Solvents in Lipase Activity. *Appl. Biochem. Biotechnol.* **2016**, *179*, 485−96.

DOI: 10.1021/acssuschemeng.9b05874
ACS Sustainable Chem. Eng. 2020, 8, 1068−1086